The University of Vermont
DEPARTMENT OF GEOLOGY
DELAHANTY HALL
180 COLCHESTER AVENUE
BURLINGTON, VERMONT 05405-1758
(802) 656-3396
FAX (802) 656-0045

March 30, 2014

Dear Dr. White:

We are pleased to submit for your consideration our fully revised manuscript. The manuscript has been extensively edited and approved for submission by both authors.

The reviews you solicited were quite useful, providing feedback and suggestions that we used to strengthen and clarify the arguments in the paper. In our *response to reviewers* document, we illustrate for each reviewer comment the specific changes we made to the manuscript. In response to the reviews, we made numerous minor changes to the manuscript which improved the clarity and broad accessibility of our presentation. Below we describe several systemic changes we made to the manuscript.

- At the suggestion of the reviewers, we carefully analyzed the relationships between the lithostratigraphy and sedimentation rate of the core and the ^{10}Be concentrations we measured. This was an illustrative exercise which clarified the active processes involved in changing ^{10}Be concentration over time; the results of this analysis are now included in the revised manuscript.
- In response to the reviewers' comments, we now more clearly articulate the assumptions underlying our interpretations and we present our interpretation as the one most consilient with the data while, at the same time, presenting alternative hypotheses.
- In response to reviewers' suggestions, we have combined and altered figures to improve the clarity of presentation.
- Per your suggestion, we have expanded the methods section and added five extended data tables and one extended data figure.

We hope that the revised manuscript meets with your approval and look forward to sharing this work to the broader community of scientists for whom we believe it will be important.

Sincerely,

Paul Bierman, Professor of Geology and Natural Resources

Response to reviewer's and editor's comments – Bierman and Shakun

Original comments in normal font
Responses in italics

Referee #1 (Remarks to the Author):

The paper 'Cosmogenic ^{10}Be records 10 million years of Greenland Ice Sheet history' by Bierman and Shakun is very interesting. The use of ^{10}Be to deduce the evolution of the Greenland ice sheet is very innovative and the results reached are in agreement with the common understanding of the evolution of the Greenland Ice Sheet.

Some ma[y]or points:

The sedimentation rates as reported on figure 3a (from table 1 and table 3) could be included more in the discussion in the paper.
Based on the reviewer's comment, we now mention the sedimentation rates in the manuscript in three places; this comment was very useful because the sedimentation rates buttress the arguments we make based on ^{10}Be. We do not focus further on sedimentation rates due to space constraints and because the goal of our research was to do the ^{10}Be isotopic stratigraphy of the core which still provides the canonical long-term history of the Greenland Ice Sheet (the core used by Larsen et al in their 1994 SCIENCE paper). We have tried to make this last and important point more clear in the manuscript.

a) The sedimentation rate seems constant for the period 2-0 ma (depth 0-100m; rate 5 cm/ka)
This information now incorporated into manuscript per the above response

b) Below 90 m (90-300 m) the determined ages from table 3 are nearly statistically the same all with very big error bars. It is possible to find dated values that are not consistent with the fitted age depth relation (on figure 3a) and to find sections with equal age. Is it quite certain that the chronological stratigraphy is undisturbed?
The large age error bars over this depth interval primarily reflect the relatively weak slope in the global strontium-isotope curve during the Pliocene, which means that a given strontium-isotope measurement on foraminifera in cores from 918 (those we analyzed for ^{10}Be) cannot be precisely dated using Sr (since measured Sr data overlaps with the global curve at more than one time when measurement uncertainties are considered). This uncertainty, therefore, is one of absolute age, but not relative age (i.e., the internal stratigraphy is in order). For

instance, as the authors of the site 918 strontium-isotope stratigraphy note, "there are no reversals and no indications of major gaps in the planktonic Sr-isotope record" (Israelson and Spezzafarri, 1998). The initial ODP report as well as Larsen et al. likewise do not suggest any evidence that the stratigraphy is disturbed. The age-depth curve fitted through the age control points is derived from a published Bayesian age modeling program that seeks a best-compromise between all available data without violating stratigraphy, and it appropriately computes a large uncertainty range over this interval, which we take into account in our Monte Carlo simulations of the ^{10}Be record shown in Figure 3c. Although the best fit age model for site 918 has uncertainty it is sufficiently robust to address the first-order ice sheet history questions discussed in the manuscript.

c) In the depth 90-300 m (ages 2-2.5 ma) the sedimentation rate is high (30 cm/ma) and in Larsen, 1994 (ref 10) it is pointed out that in the depth zone 100-170 m the highest concentration of IRD are observed.
This information now incorporated into manuscript per above response.

I find that these sedimentation observations could be used and might strengthen the argumentation in the paper. The fact that the 0.8 ma decrease of ^{10}*Be* is not at the boundaries of the sedimentation rate changes is also worth observing.
The reviewer's observation of the lack of sedimentation rate response to the decrease of ^{10}Be concentration is an important one. The ms. is now strengthened incorporation of these data.

The figures could use some rework.

Figure 1 and figure 2 are less informative than 3 and 4. Perhaps they could be merged?
We agree with the reviewer and have merged figures 1 and 2; they are now part of a two panel figure.

Figure 3 The shaded error-zone on figure 3b is too week. The line from 324 cm to 386 cm in figure 3b where no data is present should be removed or be shown as a dashed line.
We have made these corrections.

I would include an extra figure with a blow up of the time zone 2.4 - 0 ma as most data and most conclusions are from this time period.
We have added a blow up of the last million years to the final figure (Figure 3).

Figure 4 (the figure used for the conclusion in the paper). Figure 4a. It is unclear if the sand concentrations are in points or averages over zones.
The sand concentrations are points and we have added that information to the caption as well a binning the sand data so they are directly comparable to the

^{10}Be data. This is now figure 3b.

Also it is unclear where they are published (Larsen, 1994?).
These are data from our sample preparation work; we have added the data to the supplement and made the source of the data clear in the figure caption.

Is it possible to make the plot of the data more usable for interpretation (a blow up of 2.4 - 0 ma would help). Figure 4b. remove or dash the tilting line with no data as in figure 3b.
We have made these changes.

The shaded error zones are too week. It would help the interpretation if vertical shaded areas over zones of interest are included (like 0.8 - 0 ma; the peak 2.2 - 2.4 ma; the minimum 2.6 - 2.8 ma and the peak 0.25 - 0.33 ma).
We have made the error zones more distinct and have added vertical guidelines every 2 Myr to the plot to help the eye find the various features we discuss in the text. We experimented with highlighting the zones of interest, but this seemed to make the plot too busy.

Minor comments:

Page 5 line 103-107 From figure 4 it is not statistical clear that there is a decrease in the decay-corrected ^{10}Be from 4.7 to 0.8 ma.
We have revised the text to be more accurate

Page 5 line 109 nearly 150.000 atoms/g - why not mention the observed values from table 1 (126.000 atoms/g)
We have changed the stated value to > 10^5. We refrain from inserting 126,000 because of the ^{10}Be and age model uncertainty.

Page 6 line 117-118 According to the argumentation on page 7 line 147 a rate of atoms to tens of atoms per gram per year would actually make it possible to create the needed rate at 2.4 ma with a ice free period of 20.000 years as reported from Kap Koebenhavn
This is a point we considered at length when preparing the manuscript. The Kap formation is not directly dated and there are no robust constraints on its duration, simply an assumption that deposition occurred over at most half of a glacial cycle (Funder et al., 2001). In response to this comment, we have added more information about the Kap formation to the text and we have elaborated on the result of sediment mixing during erosion and its effect on isotope concentration. We have added wording that the deglaciation which deposited the Kap is an explanation for this spike in ^{10}Be concentration at 2.5 My.

Page 6 line 119 Again - the decline from 2.5 to 0.8 ka is not clear from figure 4
We have revised the text to be more accurate; only the peak values decline.

Page 6 line 126 to Page 7 line 142: I believe this is where the sedimentation results could strengthen the discussion. I find the most likely explanation is the change from a 41 to a 100 ka world around 0.8 ma. During the 41 ka world the waxing and waning a smaller ice sheet would give higher ^{10}Be concentrations than from the larger ice sheets in a 100 ka world.
It is unclear if the Greenland Ice Sheet was smaller during the 41 kyr world. The marine oxygen isotope record reflects ice volume but not extent, and tills from mid-continent North America suggest that the Laurentide was at least sometimes as extensive during the 41 kyr world as the 100 kyr world. One other challenge here is that the whole Greenland Ice Sheet can only account for ~0.05 per mil changes in marine d18O due to its small volume, which barely exceeds the noise level in the record. We think the reviewer's point is a good one though, and have added the reviewer's thoughts as an alternative hypothesis that the higher ^{10}Be in the 41 ky world could be due to a generally smaller ice sheet, in addition to our previous suggestion that the ice sheet may have deglaciated more frequently.

I find the arguments on CO2 and Temp on page 7 lines 140-142 to be badly justified. If kept they should be under-built with a few sentences more.
If the ice sheet was smaller during the 41 kyr world as the reviewer suggests (and we agree that is a possible explanation for our data), then it follows that the ice sheet was sensitive to modest warming because many proxy records show that the early Pleistocene was not much warmer than the Holocene. We have rephrased this section to make our argument more clear – we do not have space in the manuscript to elaborate further.

Page 7 line 145 The Mid-Brunhes spike could be discussed in relation to the most likely candidates for retreat of the Greenland ice Sheet - the interglacials MIS 5 and MIS 11.
Uncertainty in the age model prevents us from identifying with great confidence which MIS the spike is related to. We have added speculative correlation to the manuscript that the spike is MIS 11, and include the d18O record we generated which, although it is low-resolution, clearly indicates the ^{10}Be spike predates MIS 5 and probably postdates MIS 11. We have added these data to what is now figure 3 and discussed them in the revised manuscript.

Referee #2 (Remarks to the Author):

Confidential comments to the authors:

The paper by Bierman and Shakun provides to my knowledge the first record of in situ-10Be from a marine sediment core. The uniqueness lies in the ability to

measure these very low nuclide concentrations in small sample volumes containing little sand derived from the Greenland continent. For this more analytical reason, the Earth science and cosmogenic nuclide community has not yet been able to provide rates of landscape change over time from such cores.
We thank the reviewer for acknowledging the unique nature of the data set.

Without doubt, there is a lot of potential in applying this method to sediment cores, one of the potentials being the reconstruction of Earth´s sedimentation- and associated CO2 withdrawal history. However, in my opinion the potential lies at constraining rates of landscape change through the past, via paleo-erosion rates, and not in reconstructing ice sheet evolution with doubtful interpretation as it is done here.
For Greenland, because it has been glaciated through at least the Pleistocene, we can only calculate paleo-erosion rates for sediment preserved from the dawn of glaciation. We agree with the reviewer that the approach we take could be applied fruitfully elsewhere and have revised the manuscript to indicate the wide applicability of the method we demonstrate here as a proof of concept.

I say this for the following reasons, which at the same time yield enough doubt on this approach to vote against publication of this work in Nature:

1) I have serious doubts that the model presented by the authors can work that way. The conceptual framework itself is all right, that is that an ice-free landscape builds up nuclides, growing ice caps first remove nuclides and then no nuclides are exported anymore due to complete shielding from cosmic rays
We are unclear about what "that way" means (so cannot respond to that comment) but we agree with the reviewer that the conceptual framework is sound. It was the foundation on which the proposal to make these measurements was based and we believe that it is the reason the isotope record is coherent containing both long-term trends and variability at the times one would expect (the dawn of the Pleistocene and the transition from the 41 ky to 100 ky world).

However, important points are not touched at all. To name the most important ones, the same or a similar pattern of nuclide export could result simply by eroding (or shielding under ice) different areas of Greenland, thereby producing at times lower nuclide concentrations or at times higher nuclide concentrations when areas not covered by ice are eroded.
We disagree with reviewer that the isotopic record could be the result of a random distribution of ice and erosion on Greenland over time. Our disagreement is based on the coherence of the overall record (the general decline of ^{10}Be over time, the spike in ^{10}Be at the dawn of the Pleistocene when other records also indicate massive expansion of the ice sheet, and the isotopic

response at 0.8 My to the change from 41 to the 100 ky world). The coherence of the ^{10}Be record is further buttressed by its agreement with other records shown in figure 3 – specifically, ^{10}Be concentration changes are mirrored in the stable isotope record and the IRD record as reflected by sand concentration in the sediment we analyzed. In response to the reviewer's comment, we have made these arguments more clear in the text.

Or the nuclide concentration that is recorded in the core may be derived from areas of Greenland most proximal to the core, permitting no conclusion about its overall glaciation history.
This comment was useful as it made us realize we did not articulate well enough in the manuscript our thoughts on sediment sourcing. In light of this comment, we have revised the manuscript to indicate that the sediment carried offshore and deposited at the coring site comes from a specific "ice shed", that is the area of the ice sheet from which the ice flowing to the continental margin is eroding its bed. The ice shed extends from the ice divide to the coast. While the core record does not indicate the history of the entire ice sheet, it does indicate the history of the southeastern sector of the Greenland Ice Sheet, much like the original IRD record (Larsen et al., Science, 1994) from this core. We have addressed the reviewer's comment by adding that caveat to the manuscript. Our work onshore tracing interglacial sediment sources (Nelson et al., in press) indicates that even during interglacials, most sediment filling the fiords (the material that will be carried offshore as IRD in the next glacial advance) is sourced from below the ice). In further response to this comment, we have added specific reference to the Nelson et al paper and its conclusions in regard to sediment sourcing.

I suspect that the authors would agree to this criticism, as they did not provide any variance, but only a mean, for the modern cosmogenic
nuclide data measured at three locations in southern Greenland (referencing to a Master´s thesis which cannot be checked). If they gave a variance, would this include much of the variability of the past several million years in 10Be concentrations?
At the time of initial submission of this paper to Nature, the data of concern to the reviewer were in review with ESPL and could not be cited except for the MS thesis. That paper (Nelson et al.) has now been accepted and is in press and thus now cited in this (the Nature) manuscript. In response to the reviewer, we have added data to the figure in question (figure 3c), which shows that the concentration range of ^{10}Be in modern Greenland sediments lies almost entirely within the range of the late Pleistocene and contain less ^{10}Be than sediment leaving Greenland during earlier times.

Secondly, concepts like "cold-based ice" and warm-based ice" are entirely neglected by the authors, thereby crucially oversimplifying their model. Cold-based ice does not maintain high erosion rates but rather protects the ground

from being eroded. Warm-based glaciers remove bedrock, but here it is important to estimate the depth of erosion, as the nuclide "clock" might not be reset entirely.

We thank the reviewer for pointing out the basal conditions consideration. In the original manuscript, we were remiss in not being explicit in our consideration of warm and cold-based ice. In response to this comment, we have revised the manuscript to indicate that most sediment delivered offshore is eroded from areas where ice was at some point in time warm based. The comment about depth of erosion puzzles us. Our conceptual model (the schematic, figure 1a) explicitly considers erosion depth over time. That "lack of resetting" and on going erosion is the basis for our interpreting the overall decline in the decay-corrected ^{10}Be concentration over time. If erosion were deep enough to totally "reset the clock" there would be no record to interpret. We have added some words to the manuscript to indicate more clearly that erosion is insufficient to remove all nuclides in the hope that this addresses the reviewer's comment and makes our thinking more clear to other readers.

For example, the authors interpret the very low nuclide concentrations measured at 2.7 Ma to be a signal of "progressive glacial erosion during late Pliocene times" (l. 101 ff., where, btw, the increase in coarse sediment could be due to lower preservation potential in older record parts), but the same signal could also be produced by a thick, warm-based ice cap that exports some sediment containing very little (because shielded by ice) nuclides.

We agree with the reviewer here that the signal reflects sediment export from a large ice cap – but wonder based on this comment and the one above if we have not been clear enough about the presence of ^{10}Be deep below the pre-glacial landscape because of production by muons under the relatively stable, pre-glacial (Pliocene/Miocene) landscape. It is that muon-produced ^{10}Be that is present at thousands of atoms/gram and which is exported after the shallow regolith (containing high concentrations of ^{10}Be) has been eroded and exported. To address this misunderstanding, we have added a more specific explanation to the manuscript and we have added an illustrative, schematic 50 meter-thick depth profile of ^{10}Be concentration to Figure 1a.

I am saying that these signals are not entirely tied to single events, but rather reflect a combination of -ice thickness and ice features, -duration of interglacial exposure, - inheritance taken over into the next glacial cycle, area eroded, region eroded (altitude of eroding region governing nuclide production) and so forth. A sensitivity analysis containing these parameters, their change with time and response times would be needed to support the suggestions made by the authors, but as is the observed "pattern" of nuclide concentration changes cannot be linked to changes in glaciation history.

We completely agree with the reviewer that the isotopic signals we see in the record reflect the sum of numerous processes acting over a variety of spatial and

temporal scales and have tried to reflect this subtlety in our revision of the manuscript. In response to this comment, we have added such a statement to the manuscript; yet, the overall pattern of the isotopic record we present is coherent indicating substantial changes in isotope concentration at times in the past where many other records indicate shifts in the climate and cryospheric systems. We have made wording changes to better articulate this in the manuscript. We disagree with the reviewer that a formal sensitivity analysis would shed more light on the system. The community's knowledge of the parameters suggested for such an analysis is so fragmentary that the results would be unconstrained. Our manuscript presents a unique data set and what we consider to be the most parsimonious explanation of those data given what the community knows today. In response to this comment, we now clearly state in the manuscript that ours is not a unique explanation; rather it is the explanation that is "most consistent" with the data given our current understanding of climate and glaciologic changes over time.

2) What the authors have not looked at (and not even mention as possibility) is the change in nuclide production rates due to changes in the intensity of Earth´s magnetic field and solar activity that could govern the overall magnitude of nuclide concentrations in contrast to ice sheet changes. Since overall nuclide concentrations are very low but production rates are high, a shift to a production rate being higher by 20% or lower by 20% relative to today´s production rate will make a large difference. Moreover, since periods of e.g. reduced solar activity cause cosmic radiation to be reduced, thereby causing to some extent ice sheets to grow or vice versa, there is a feedback to this that needs to be looked at in detail. Thus, albeit one must note a correspondence between the overall magnitude in nuclide concentration (high versus low) and the evolution of the Greenland Ice Sheet (ice-free versus ice-covered), this "agreement" could be ruled by the intensity of cosmogenic nuclide production. The exact mechanisms need to be described first conceptually, so that an increase or decrease in nuclide concentrations can be attributed to changes in ice sheets, and not to changes in nuclide production rates.
We thank the reviewer for pointing out that we did not explicitly address production rate changes in the manuscript. We have now indicated in the manuscript that production rate changes due to magnetic field changes are unimportant. The reason – a large and well-established literature going back to Lal and Peters (1967) indicates unambiguously that cosmogenic production rates at high latitude sites (>60 degrees, which includes all of Greenland) do not change in response to magnetic field variations over time.

3) I have several issues with the age model. I am aware that we are dealing with relative changes in nuclide concentrations and that we are not talking about changes that happen overnight, therefore only a very crude age model would be sufficient. The age constraints using Sr in marine carbonates and biostratigraphy

do not give an absolute age but rather a depositional age of the terrestrial sediments.
We agree with the reviewer that even a "crude" age model would be sufficient; the model developed for site 918 is much better than crude and thus sufficient for the conclusions we draw. We don't understand the reviewer's second comment. The Sr-isotope and biostratigraphy do provide ages for sediment deposition anchored in absolute time, and despite substantial uncertainty around each data point, the age of these sediments across late Cenozoic epochs is not in doubt.

This is a problem especially for the older parts of the core where dating from magnetic reversals are absent (why are uncertainties on ^{10}Be concentrations from Monte Carlo similar for today and e.g. 5 Ma ago? Should they not increase with age as the associated uncertainties are also increasing with age?).
The point the reviewer raises here reflects an omission on our part that has now been corrected in revision. Indeed, the uncertainties at 5 Ma are larger than today, but they look similar at first glance because the plot is on a log scale – we have now specifically noted that the graph is logarithmic in the caption which should reduce the chance of readers being confused. The gray error window is fairly large during the late Pleistocene because the ^{10}Be spike a few hundred thousand years ago slides around in time in the monte carlo simulations; thus the error window reflects the possibility that the spike could occur at 0.7 Ma or 0.2 Ma; however, stable isotope analysis of forams in the same sediment from which we extracted quartz for ^{10}Be analysis indicates that the peak likely occurs shortly after MIS 11, better constraining the model.

One other problem is that sediment transport from the coast to the core location (100 km at depths of 1800 m) may take very long, thereby obscuring the chronology.
Our reading of the Larsen et al. 1994 SCIENCE paper on this same core as well as the shipboard reports describing the core suggest that much of the material we analyzed is ice-rafted debris. This suggests transport by icebergs from calving ice margins to the core site occurred relatively quickly (years to decades) and thus did not obscure the chronology through long coast-to-coresite transport. In any case, even long transport lags over glacial cycles would not have much effect at the time scales discussed in the manuscript (hundreds of thousands to millions of years). In response to this comment, we have added specific wording to the manuscript about sediment transport time and the predominance of IRD in the sediment we analyzed.

Therefore, the statement of the authors that "age model uncertainties can alter the absolute value of decay-corrected ^{10}Be concentrations and ...., but have minimal impact on the overall structure of the record" does not apply. The "dating" of older parts of the record could be heavily biased towards wrong ages and this should be visible by increased ^{10}Be uncertainties for very old samples.

Working with a previously dated marine core, we depend on the work of others for the age model. However, the nature of this comment makes us suspect that the reviewer missed the log scale on figure 3c. e.g., the oldest sample error spans nearly 500,000 atoms/g, while late Pleistocene errors are one to two orders of magnitude smaller. We have now pointed out the log scale in the caption with the hope of making it more clear to readers.

Referee #3 (Remarks to the Author):

First, let me say that this is a beautifully simple idea. The highest compliment I can pay is that I wish I had thought of it myself. Masking the landscape with ice should gradually decrease the amount of ^{10}Be in the sediment that is eroded, and the concentration in sediment offshore should indicate in the broadest sense the presence or absence of glacial cover. The idea is original and significant (although similar in some ways to Balco's work on continental till from the Laurentide ice sheet).

There are several issues that are not addressed, but should be. The first is the possible influence of cold-based (non-erosive) ice. We know from several studies at high latitudes that there are deglaciated surfaces that still maintain relatively high concentrations of ^{10}Be despite being previously covered by ice. How would this affect the ^{10}Be concentrations in the sediment? I suspect it is not a problem for two reasons: the long time periods imply that radioactive decay will lower concentrations under the ice, but more importantly the presence of sediment itself implies that it is derived from erosive ice.
We thank the reviewer for pointing out our oversight (not mentioning cold vs. warm based ice) in the initial draft of the manuscript. In response to this comment and a similar comment by reviewer 2, we have added specific wording about basal thermal conditions and their effect on sediment sourcing to the manuscript.

I am by no means a specialist on Greenland or on sediment cores, but as I read through various papers on the cores being analyzed, I was left wondering why the authors did not correlate their measured ^{10}Be to the observed lithofacies.
We again thank the reviewer for their insight and have added panel A to Figure 3 that indicates the lithofacies.

Most who have analyzed that core have noted that there are gravel layers, sandy layers, and diamictons interspersed with more normal marine sediments. In particular, the zone near 250 meters depth where the authors see a drastic change from low to high ^{10}Be concentrations seems to correlate to the upper boundary of the thickest diamicton. Is the low concentration near 2.7 Ma just the

^{10}Be concentration in the diamicton itself? That is, does this sample directly record the concentration in glacial till? Is the rapid variability in the Quaternary due to various lithofacies being sampled? This is the very same zone where others have observed alternating diamictons. Even in the Pleistocene there is order-of-magnitude variability from sample to sample. Before drawing grand conclusions about the coverage of all of Greenland by ice, I think it would be useful to explain more clearly the provenance of the various samples, at least at the level of correlation with previously described lithofacies. It is important to understand the source of the sediment.
This is an insightful comment and has led us to consider (and add wording to the manuscript) the influence of lithofacies on ^{10}Be concentration. There are five packages of coarse material identified in the core by Larsen – each of these five large packages (shown in figure 3a) correlate with lower ^{10}Be concentrations and we have now added this observation to the ms. We interpret this drop in ^{10}Be as the effect of glacial erosion – quarrying material from depth. We thank the reviewer for helping us to correct this omission in the initial draft of the manuscript.

Small errors, suggestions, and questions:
'Aerially' is misspelled in the abstract (line 24).
Fixed

Change to 'several meters of rock or ice', line 52.
Fixed

Line 114-how long would deglaciation have to last to produce the observed increase?
We are not comfortable providing a duration because erosion depth is not constrained. Shallow erosion would require less time of exposure than deep erosion.

Lines 132-135-exactly how do your results support the regolith hypothesis? I would be more convinced to see evidence from, for example, clay composition. The conclusion seems a stretch.
We offer the suggestion that these data may support the regolith hypothesis as a testable hypothesis/alternative explanation rather than as a conclusion. If the ^{10}Be drop was due to a shift in erosion of regolith to bedrock (as opposed to other explanations mentioned for the ^{10}Be drop, such as a buildup in ice cover), its synchronicity with the mid-Pleistocene transition is in line with the regolith hypothesis, which argues for just such a substrate shift at this time, albeit in North America. We have rephrased this sentence to make it more speculative and to make our assumptions more clear.

Lines 139-141-this idea could be tested by measuring ^{26}Al together with ^{10}Be.

This would be great to do and we have considered making these measurements. The problem is, the ^{10}Be measurements were difficult enough to make; with ^{26}Al beam currents more than an order of magnitude lower and considering the shorter half-life of ^{26}Al, such measurements aren't likely to be meaningful until AMS technology improves.

Line 169-if your sample spans 3.1 My (line 163), it seems inappropriate to decay-correct using the average age.
We have considered this comment and re-examined the sand distribution data. We find that sand comes from across the interval and thus we conclude that decay correcting the average age is okay to the first order.

Figure 4-the sand abundance data is not properly cited.
Thanks for pointing this out. We have responded to a similar comment by reviewer 1 and now cite the source of those data and include them in the supplement.

To summarize, I think the authors have come up with a fantastic and novel data set that is worthy of publication in a high-profile journal such as Nature. I suspect that there may be more useful information lurking within the data, and I encourage the authors to explicitly discuss or explore how ^{10}Be varies with lithofacies. This might help lend some support to the conclusions, which at this point are perhaps not as robust as they could be.
We thank the reviewer for their suggestions.

Editors comments

The referees indicate three main problems.

First, you have not adequately considered alternative explanations.
On the basis of constructive reviewer criticisms, we have added further discussion to the manuscript text which addresses alternative explanations including the effect of cold/warm based ice, magnetic field forcing of ^{10}Be production rates, and the effect of lithofacies changes on isotope concentration – all of which we feel make the paper more complete and the conclusions more robust.

Second, the age model is not sufficiently robust.
We think that the age model for the core is reasonable and more refined than it was when the Larsen et al paper was published by SCIENCE 20 years ago – in addition to the magnetic reversals and biostratigraphy Larsen et al used, we also include a published Sr-isotope chronology for the past 10 million years and our

own foram d18O data for the last one million years. Our ^{10}Be analysis is the first significant addition to the Larsen story about 918 (which has stood well the test of time) and remains the canonical record of ice sheet development on Greenland. While cores with better age models exist, they are farther off shore and do not have enough quartz sand for ^{10}Be analysis. We feel strongly that site 918 has good enough dating for us to paint a picture of long-term Greenland Ice Sheet history that both verifies and goes beyond the initial interpretations of Larsen – even reviewer two, who is critical of the age model, agrees that it is sufficient for the science we are doing in this paper, especially for the last two million years where we have magnetic reversals.

Finally, it is not clear that the changes you propose are supported by firm statistical evidence.
In response to the reviewer's suggestions, we have conducted several statistical tests. We have performed a regression considering the decay-corrected ^{10}Be concentrations over time and show there is a statistically significant decline in ^{10}Be over the duration of the record. We have added this information to the manuscript. We have done an ANOVA on the ^{10}Be data from 10-2.5, 2.5-0.8, 0.8-0 Ma as well as the data of Nelson et al and find that the early and late Pleistocene are clearly separable populations (p=0.003), the Miocene/Pliocene is not statistically different than the early Pleistocene (p=0.28) and that the late Pleistocene and contemporary populations are similar (p=0.16).

That said, even though the concerns are serious (especially those from referee #2), the referees suggest seemingly clear paths forward, such as sensitivity and lithofacies analyses.
We agree that lithofacies analysis was the right thing to do. We did it and it improved the paper and the robustness of our conclusions. A sensitivity analysis, in the manner suggested by reviewer 2, does not make sense to us because the parameters the reviewer suggest we test are poorly if at all constrained. Such a poorly constrained model would add little, if anything, to our existing interpretation.

Consequently, should further data, theoretical analysis and/or lines of argument allow you to address these and all of the other criticisms -- and you still reach a new and important insight into the history of the Greenland Ice Sheet -- we would be happy to look at a revised manuscript (unless, of course, something similar has by then been accepted at Nature or appeared elsewhere).
We thank you for considering our revised manuscript and hope that you find our revisions satisfactory.

For submission to Nature as a letter, revision after review

March 29, 2014

Cosmogenic ^{10}Be records 10 million years of Greenland Ice Sheet history

Paul Bierman, Department of Geology and Rubenstein School of the Environment and Natural Resources, University of Vermont, Burlington, VT 05405, pbierman@uvm.edu, 802 656 4411

Jeremy D. Shakun, Department of Earth and Environmental Sciences, Boston College, Chestnut Hill, MA 02467, jeremy.shakun@bc.edu, 617 552 1625

Clastic marine sediments preserve material eroded from the continents, allowing the development of time-series that quantify the character of now-eroded landscapes, including the growth of ice sheets. Sediment from non-glaciated landmasses typically contains high concentrations of the cosmogenic nuclide ^{10}Be, the result of exposure to cosmic rays. In contrast, ice sheet cover prevents cosmogenic nuclide production and erodes material containing nuclides produced before glaciation, decreasing the concentration of ^{10}Be in sediment carried by ice. The Cenozoic growth and erosion history of the Greenland Ice Sheet is poorly constrained. Here we use a record of *in-situ*-produced ^{10}Be in detrital sediment from a marine core off the southeast coast of Greenland to decipher the long-term history of the ice sheet. The ten-fold drop in decay-corrected ^{10}Be concentration of Greenland-derived quartz between 10 and 3 million years ago reflects limited Miocene and Pliocene glaciation and progressive erosion of material containing ^{10}Be produced before glaciation. A drop in ^{10}Be concentration ~ 2.7 million years ago indicates continent-wide expansion of the ice sheet, coincident with the onset of Northern Hemisphere glaciation inferred from marine oxygen isotope and ice-rafted debris records. A four-fold decrease in ^{10}Be concentration across the mid-Pleistocene transition reflects either the final removal of pre-glacial regolith or intensification of glaciation. By about 800,000 years ago, ^{10}Be concentration in core sediment is indistinguishable from that of sediment exported by the ice sheet today, suggesting that the ice sheet has been generally large and stable since then. Spikes in ^{10}Be concentration are consistent with interglacial exposure of the continent. This approach could be useful to reconstructing the history of other landscapes.

The long-term history of landscapes has been interpreted by analysis of marine sediment cores, which preserve in their physical, chemical, and isotopic stratigraphy a record of Earth history and both surface and marine processes including the coming and going of ice sheets[1,2]. However, relatively few proxies provide a direct, quantitative, and large-scale indicator of the variability of individual ice sheets[3]. Such information is critical to establishing the sensitivity of ice sheets to climate change, which is the largest source of uncertainty in future projections of sea level rise.

Continental glaciation of Greenland is thought to have begun near the onset of Northern Hemisphere glacial cycles at ~ 2.7 Ma inferred from marine oxygen isotope and ice-rafted debris (IRD) records[2,4,5]. Other marine and modeling data suggest initial ice mass growth in Greenland commenced from 5 to 25 million years earlier[6-8]. It is unclear how Greenland glaciation evolved once the ice sheet was established, for instance, across the mid-Pleistocene transition[9].

Beryllium-10 is produced in near-surface rock and soil primarily by the bombardment of cosmic-ray neutrons. At depths below several meters of rock or ice, ^{10}Be production is much less and is dominated for many tens of meters below the surface by muon interactions[10]. Continental sediment usually contains >100,000 atoms g^{-1} of *in-situ* produced ^{10}Be, the result of subaerial exposure to cosmic rays[11]. On a steadily eroding, ice-free landscape, the concentration of ^{10}Be in sediment can be interpreted as an erosion rate assuming the elevation and latitude of the sediment source is known[12]. Once Earth's surface is covered by glacial ice, ^{10}Be production effectively ceases and glacial erosion removes the most highly-dosed, near-surface material first before excavating material at depth containing progressively less ^{10}Be (Figure 1a). Below slowly eroding terrains, measurable concentrations of ^{10}Be extend tens of meters below the surface, making complete removal of pre-glacial ^{10}Be by glacial erosion unlikely.

After the start of glaciation, the concentration of ^{10}Be in marine sediment sourced from Greenland is determined by the ^{10}Be concentration of material eroded by the ice sheet from its bed (the former land surface) and transported to the coast. The ^{10}Be concentration on the bed is controlled by pre-glacial isotope production and landscape erosion rates and, after glaciation begins, by the rate of sub-ice erosion, the time since the bed was covered by ice and nuclide production ceased, and the duration and extent of sub-aerial landscape exposure during interglacial periods, when ice-sheet area is reduced.

In order to understand the glacial erosion history of southeastern Greenland, we measured *in situ*-produced ^{10}Be in 30 quartz sand samples from the top 554 m of Ocean Drilling Program site 918 (63.1°N, 38.6°W, 1800 m depth), located in the Irminger basin, 110 km southeast of Greenland (Figure 1b, Extended data Table 1). This site is adjacent to the more dynamic southern portion of the Greenland Ice Sheet, as suggested by modeling[13,14], and thus is well situated to record past ice sheet variability. We chose Site 918 because its physical stratigraphy has, for two decades, provided the canonical record of Greenland Ice Sheet history[8]. Based on the earliest occurrence of IRD, which is included in our oldest sample (Figures 2 and 3), site 918 defines the onset of Greenland glaciation at roughly 7 Ma[8]. The stratigraphy and core location suggest much of the sediment at the coring site was deposited directly by rain-out of IRD[8]; some of the sediment was likely deposited by mass flows but several lines of argument suggest that the quartz we measured is predominantly of Greenlandic origin, including the proximity of the core to Greenland; currents in the area drift ice from northeast Greenland (Figure 1b); site 918 is well north of the heart of the Laurentide IRD belt as reflected in Heinrich layers[15]; downcore IRD is similar to modern Greenland IRD[8]; site 919, located only 70 km further offshore than 918, contains >90% less sand[8] and sediment from nearby Iceland contains no quartz.

To estimate ^{10}Be concentration at the time of sediment deposition, we decay-corrected[16] (^{10}Be $t_{1/2}$ = 1.387 Myr) measured ^{10}Be concentrations using the core age model (Figure 2, Extended data Table 2). The chronology is anchored to the paleomagnetic timescale over the Pleistocene, but less well constrained by strontium isotope and biostratigraphy in the Pliocene and Miocene (Figure 2a). Age model uncertainties can alter the absolute value of decay-corrected ^{10}Be concentrations and change the timing of some isotopic shifts, but do not impact on the overall structure of the ^{10}Be record (Figure 3c). Because Greenland lies at high latitude, variations in magnetic field strength over time do not affect ^{10}Be production rates.

Considering the dynamics of glacial erosion and sediment transport suggests that the ^{10}Be record is most likely to preserve the signal of major, long-term changes in ice sheet behavior. There is lag time between erosion under the ice, which occurs between the ice divide in central Greenland and the continental margin; this lag is likely 10^3 to 10^5 y considering ice velocities and the storage of sediment in fjords during interglacials[17] before evacuation offshore during glacials. Most sub-glacial erosion occurs where ice is warm-based and flowing quickly; thus, clastic, glacially-derived sediments, such as we analyzed, record the behavior of the most erosive areas of the ice sheet - thick, fast-moving ice streams.

Measured ^{10}Be concentrations are low, 2100 to 40,000 atoms g^{-1} (Figure 2b, Extended data Table 2). Decay-corrected concentrations are highest in the oldest sediment (~10 Ma according to the best-fit age model, 470,000 ± 38,000 atoms g^{-1}) and generally decrease over time (Figure 3c). ^{10}Be concentrations dip in the five sections of the core where coarse material (gravel or diamict) predominates (Figure 3a, Extended data Table 3). Inverting the ^{10}Be data from the oldest sediment sample and assuming that the sediment delivered to the deep ocean as IRD was stripped by glaciers at an elevation near sea-level suggests a landscape-averaged pre-

glacial Greenland denudation rate of about 7±1 m/My, lower than average basin-scale erosion rates for average polar climates but higher than polar rates of outcrop erosion[11]. Low late Miocene erosion rates are consistent with low sedimentation rates then (Figure 2a).

By the late Pliocene, decay-corrected ^{10}Be concentrations are more than an order of magnitude lower than at the beginning of the record, reaching a minimum of 12,000 atoms g^{-1} at 2.7 Ma. We interpret this decrease as progressive glacial erosion of once-stable Tertiary regolith over limited areas of Greenland, perhaps by valley glaciers or ice caps with calving margins (Figure 1a). A general increase in the intensity and/or aerial cover of glaciation is supported by rising concentrations of coarse sediment over the length of the core (Figure 3b), by increasing sedimentation rates toward the Pleistocene (Figure 2a)[8], and by an inverse relationship between ^{10}Be concentration and percent coarse fraction (Extended data Figure 4).

At the dawn of the Pleistocene, 2.7 Ma, the decay-corrected ^{10}Be concentration abruptly decreases reflecting the first continent-wide glaciation, an interpretation consistent with the abundance of IRD and % >63 μm sediment found at site 918 at this time (Figure 3a,b,c). Soon after, by 2.5 Ma, the decay-corrected concentration of ^{10}Be rises to > 10^5 atoms/g. This relatively ^{10}Be-rich quartz likely records a major deglaciation event. One such early interglacial is represented by the Kap København Formation in northern Greenland, which contains flora and fauna indicative of a relatively warm climate[18]. Between 2.5 Ma and 0.8 Ma, the decay-corrected concentration of ^{10}Be varies and the peak values decline (Figure 3c). The Pleistocene decline in peak ^{10}Be concentration is consistent with progressively deeper stripping of the preglacial landscape by sub-ice erosion during the Quaternary. As sediment and rock are removed from the landscape under the ice by erosion, material that was deeply shielded in pre-glacial times (which

contains less ^{10}Be because it was less dosed by cosmic radiation) is incorporated into basal ice and carried offshore before being deposited as IRD (Figure 1a).

An abrupt, four-fold drop in ^{10}Be concentration occurs across the mid-Pleistocene transition at 0.8 Ma coincident with a rise in sand content of sediment at site 918 (Figure 3b,c,e). There are several possible interpretations. First, if pre-glacial regolith still existed and was well-mixed beneath the ice sheet as till during the early Pleistocene, it would have had a fairly constant ^{10}Be concentration with depth. In this case, the decrease in ^{10}Be concentration at 0.8 Ma might reflect near complete export of regolith and a switch to subglacial erosion of bedrock, which would have contained less ^{10}Be than the regolith. If there were a shift in substrate beneath the Laurentide Ice Sheet coincident with that inferred here for Greenland, the ^{10}Be data reported here would support the regolith hypothesis for the mid-Pleistocene transition from 41 to 100-kyr glacial cycles, which posits that thinner, more responsive ice sheets sliding on regolith transitioned to larger, more sluggish ice sheets resting on bedrock about a million years ago[19]. Or, an increase in the erosivity of the Greenland Ice Sheet during the mid-Pleistocene transition could have reduced ^{10}Be concentrations as deeper-sourced material was rapidly exported, though sedimentation rates do not rise appreciably at this time (Figure 2a). Lastly, the Greenland Ice Sheet may have been smaller, or deglaciated more frequently during the early Pleistocene than the late Pleistocene, helping to sustain higher ^{10}Be levels through repeated episodes of interglacial exposure. If correct, this latter interpretation suggests that the ice sheet underwent substantial retreat at early Pleistocene CO_2 and temperature levels, which were only slightly higher than those during the Holocene[3,20,21].

^{10}Be values over the past 0.8 My are similar to those in sediments issuing from the western, southern, and eastern Greenland Ice Sheet margin today[17] (Figure 3c), consistent with

the existence of a large, modern-like Greenland ice sheet for most of the last million years. Given ^{10}Be surface production rates of atoms to tens of atoms per gram per year, shrinkage of the GIS during the most extensive or long-lasting interglacials should be detectable in the Pleistocene marine record. Indeed, the spike in ^{10}Be several hundred thousand years ago is consistent with extensive land-surface exposure during the long-lived MIS 11 deglaciation[22] preceded by low ^{10}Be concentration during the penultimate glaciation, MIS 12 (Figure 3e-g).

The record of *in situ*-produced ^{10}Be in sediment derived from continental glacial erosion and preserved in marine sediment is most consistent with the development of initial glaciation on Greenland from ~10 to 3 Ma, the first growth of a full Greenland ice sheet ~2.7 Ma, and a significant change in ice-sheet behavior ~0.8 Ma. The magnitude of the ^{10}Be signal as well its general consistency with other ice sheet and climate records (IRD and stable isotope, Figure 3) suggests that our approach provides a useful new tool for reconstructing other long-term ice-sheet and landscape histories.

Methods Summary

Core samples were obtained from the Bremen Core Repository. Sediments were oven-dried, massed, and then wet-sieved. The >63μm grain size fraction was massed to determine the percent coarse fraction (Extended data, Table 3). We isolated the 0.125 to 0.75 mm fraction and used weak acid ultrasonic leaching (0.5 to 0.25% HF and HNO_3) to slowly dissolve all minerals other than quartz[23]. We amalgamated quartz from subsamples taken over an interval of core until we had sufficient quartz mass (7.8 to 25.3 g) from which to extract and measure ^{10}Be reliably. Thus, samples represent the average ^{10}Be content of quartz present in core sections ranging in length from 0.6 to 91 m (median = 7 m). Age spans for samples range from 0.002 to 3.1 My.

Samples were dissolved using HF in the presence of ^{9}Be carrier produced from beryl and processed in batches of 12 including 2 full process blanks. Isotopic measurements were made at Livermore National Laboratory and referenced to standard 07KNSTD3110[24] assuming a ^{10}Be/^{9}Be ratio of 2850 x 10^{-15}. The average blank ratio (4.6±1.0 x 10^{-16}, n=6, Extended data Table 4) was subtracted from measured ratios. Using the half-life[16] of ^{10}Be and the age model for site 918, we corrected the measured ^{10}Be concentrations for radio-decay since burial on the sea floor assuming the average age of the sediment in the sampled core interval. Eighty separate sediment samples were taken from the top 50 m of the core for stable isotope analysis (Extended data, Table 5). Isotopes were measured on ~15 N. pachyderma (s) tests from the 150-250 μm size fraction at the University of Massachusetts-Amherst Stable Isotope Laboratory.

Author contributions

PB and JDS designed the experiment. JDS oversaw core sampling. PB oversaw laboratory work and made cosmogenic isotopic analyses. PB and JDS interpreted the data and wrote the paper.

Acknowledgements

Research supported by NSF ARC-1023191. A. Nelson prepared the quartz and extracted the Be. W. Shakun and M. E. Shakun helped with sediment processing. S. Zimmerman and R. Finkel provided AMS expertise. W. Hale and the Bremen Core Repository facilitated core sampling. S. Burns made stable isotope analyses. E. Portenga extracted some foraminifera.

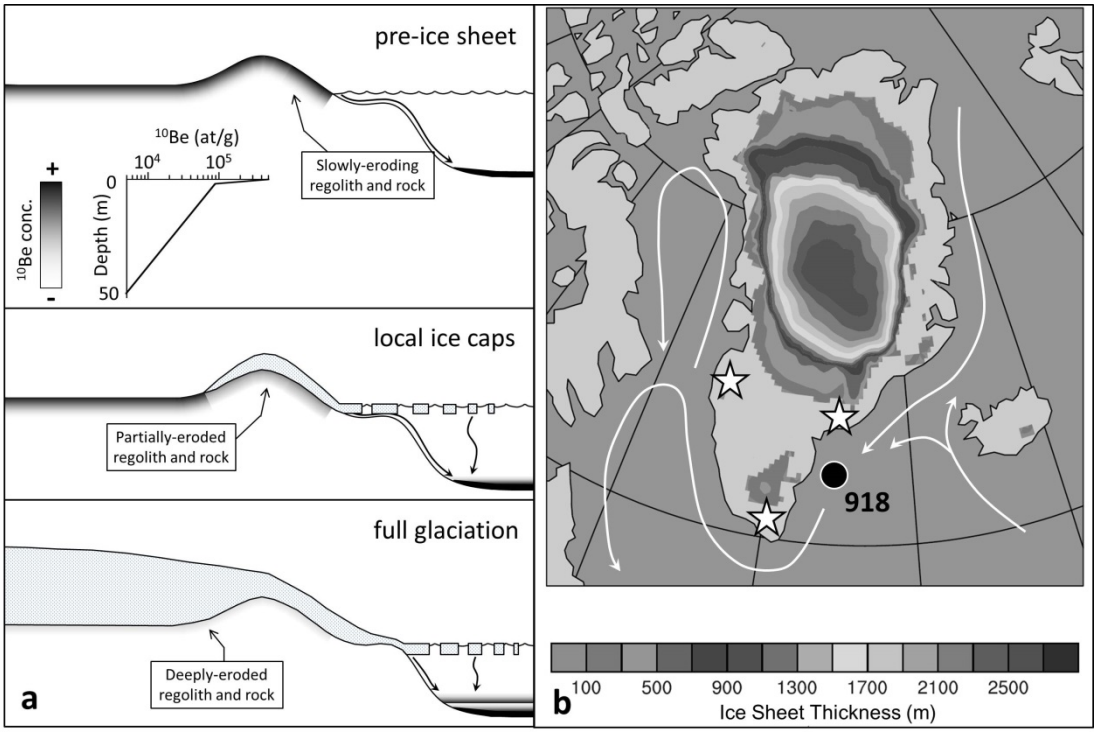

Figure 1. Conceptual model of ^{10}Be concentration under ice sheet over time and location map. (a) Ice-free conditions prior to glaciation during which low volumes of high ^{10}Be-concentration material are delivered to the ocean (top). Mountain glaciation and ice cap development during the late Miocene and Pliocene, erode and export progressively deeper, and thus ^{10}Be-poorer, material from these regions (middle). Expansion of a full Greenland Ice Sheet during the Pleistocene, initially strips previously exposed, ^{10}Be-rich surface material, then erodes progressively deeper and thus ^{10}Be-poorer material from Greenland (bottom). Intensity of shading corresponds to relative ^{10}Be concentrations in bedrock, regolith, and sediment. Top panel inset shows pre-glacial steady-state ^{10}Be depth profile assuming 7 m/My erosion rate and sea-level production rate. **(b)** ODP site 918 shown as black dot, modern ocean currents indicated by arrows, and contours on Greenland give ice sheet thickness during the last interglacial as simulated by a multi-model ensemble[25]. Stars show the locations of ^{10}Be measurements made on modern sediments[17].

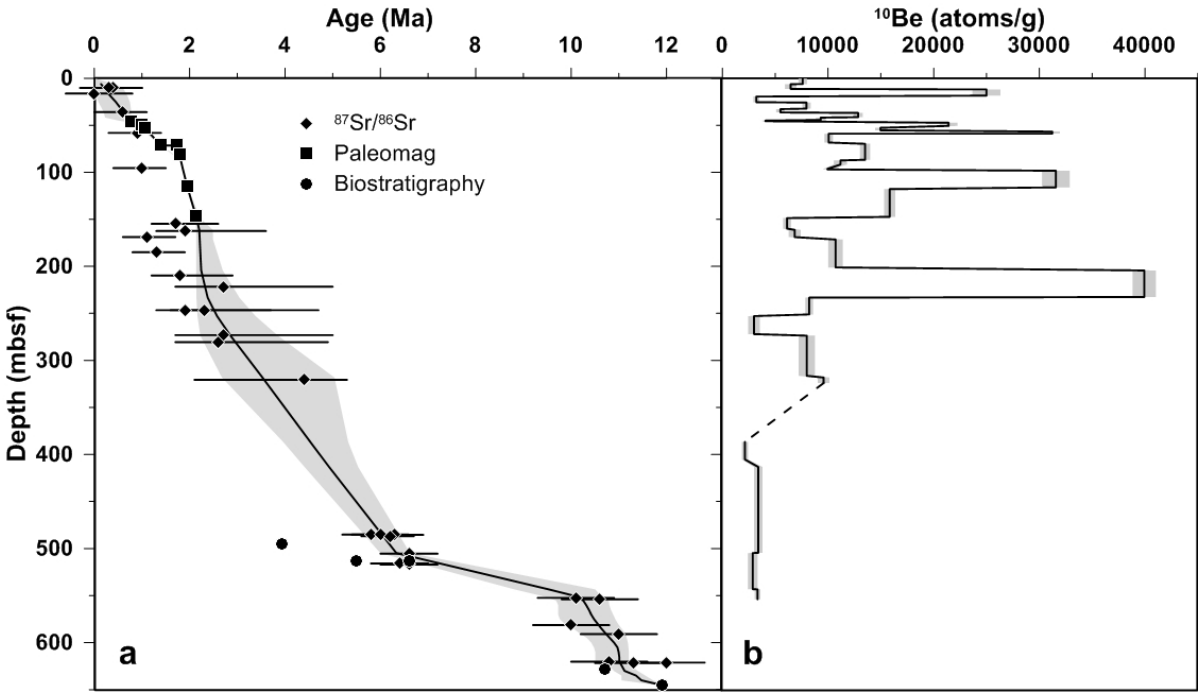

Figure 2. Site 918 age model and measured ^{10}Be concentrations. (a) Age constraints from strontium isotope[26], paleomagnetic[27], and biostratigraphic[8] data. Age-depth curve (black line) and 2σ uncertainty (gray shading) were calculated using a published age model algorithm[28]. (**b**) Measured ^{10}Be concentrations with 1σ analytic uncertainty (gray shading).

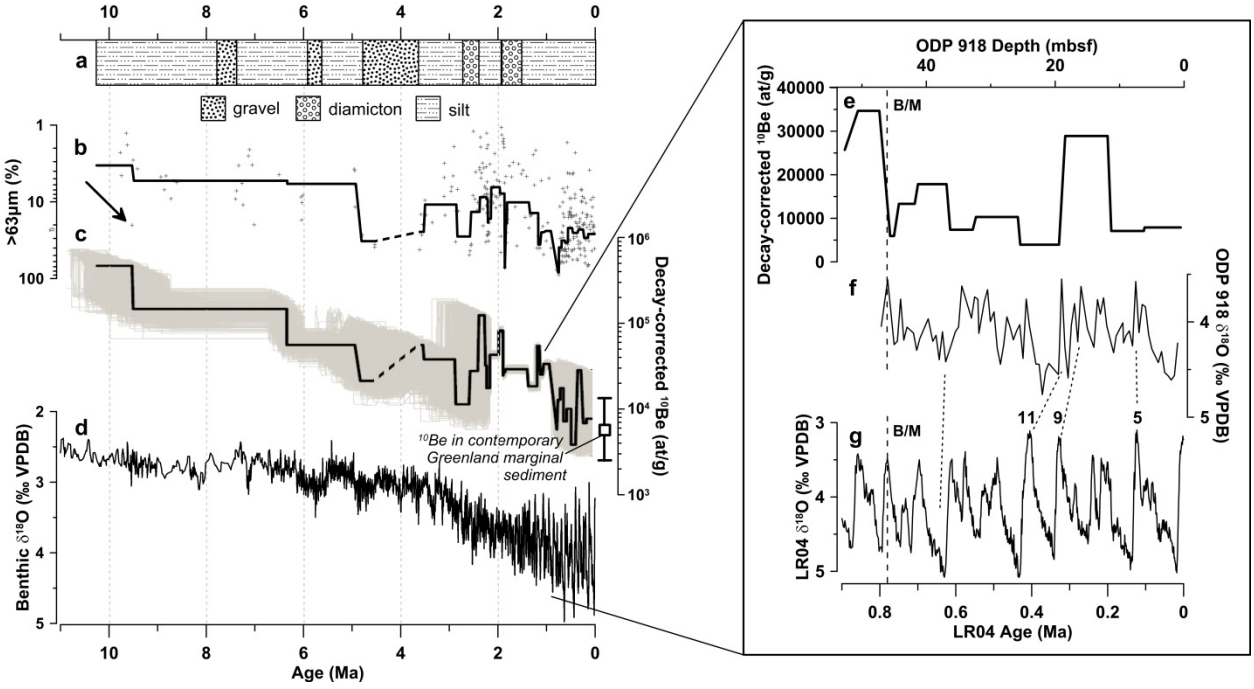

Figure 3. Site 918 decay-corrected ^{10}Be record compared to other core analyses. (a) Lithostratigraphy of core[8]. (**b**) Coarse (>63 μm) fraction (inverted, log-scale) at site 918 by weight measured during individual sample preparation for this project (see Supplementary Information). Individual samples are shown as gray dots; the black line gives averages binned in the depth ranges spanned by ^{10}Be samples. Arrow points to lowest (oldest) sample (918-30) with IRD at site 918[8]. (**c**) Decay-corrected concentrations (log-scale) of ^{10}Be measured in quartz isolated from site 918 assuming age model shown in Figure 2a. ^{10}Be concentration decreases at ~30,000 atoms/g per million years, R^2=0.62, p<0.001. Gray lines show results of 1000 Monte Carlo simulations perturbing age model with chronological uncertainties and measured ^{10}Be concentrations with analytical uncertainties. The open box next to the y-axis shows the median and 10th to 90th percentile range of ^{10}Be concentrations measured on 62 modern ice-contact and fluvial sediment samples collected from three regions of Greenland[17]. ANOVA on data from 10-2.5, 2.5-0.8, 0.8-0 Ma and modern sediment[17] shows early and late Pleistocene are clearly

separable (p=0.003) and that the late Pleistocene and modern sediment ^{10}Be concentrations are similar (p=0.16). (**d**) Global deep ocean δ^{18}O, a proxy for global ice volume and deep ocean temperature[1]. (**e**) Decay-corrected ^{10}Be concentrations and (**f**) foraminiferal δ^{18}O (N. pachyderma (s)) in the top 50 m of site 918 plotted against core depth. (**g**) The LR04 benthic δ^{18}O stack[29] plotted on its own timescale. The Brunhes-Matuyama (B/M) boundary is shown by the dashed lines at 45.9 mbsf for the site 918 data and 0.78 Ma for the LR04 stack. Select marine isotope stages in the LR04 stack are numbered, and possible correlations with the site 918 δ^{18}O record are indicated by dotted tie lines.

Extended Data Figure 4. Over the past 10 Myr the decay-corrected ^{10}Be at site 918 is inversely related to coarse fraction percentage and the marine benthic δ^{18}O. The coarse fraction and benthic δ^{18}O data were averaged in bins spanning the age ranges of corresponding ^{10}Be measurements. Best-fit lines and regression statistics are shown. Note that the ^{10}Be and coarse fraction axes are log-scale.

Extended data tables and one figure are linked to the online version of the paper at www.nature.com/nature.

References Cited

1 Zachos, J., Pagani, M., Sloan, L., Thomas, E. & Billups, K. Trends, rhythms, and aberrations in global climate 65 Ma to present. *Science* **292**, 686-693, doi:10.1126/science.1059412 (2001).

2 Shackleton, N. J. *et al*. Oxygen isotope calibration of the onset of ice-rafting and history of glaciation in the North Atlantic region. *Nature* **307**, 620-623 (1984).

3 Alley, R. B. *et al*. History of the Greenland Ice Sheet: paleoclimatic insights. *Quaternary Science Reviews* **29**, 1728-1756, doi:http://dx.doi.org/10.1016/j.quascirev.2010.02.007 (2010).

4 Maslin, M. A., Li, X. S., Loutre, M. F. & Berger, A. The contribution of orbital forcing to the progressive intensification of Northern Hemisphere glaciation. *Quaternary Science Reviews* **17**, 411-426, doi:http://dx.doi.org/10.1016/S0277-3791(97)00047-4 (1998).

5 Mudelsee, M. & Raymo, M. E. Slow dynamics of the Northern Hemisphere glaciation. *Paleoceanography* **20**, PA4022, doi:10.1029/2005pa001153 (2005).

6 DeConto, R. M. *et al*. Thresholds for Cenozoic bipolar glaciation. *Nature* **455**, 652-656 (2008).

7 Eldrett, J. S., Harding, I. C., Wilson, P. A., Butler, E. & Roberts, A. P. Continental ice in Greenland during the Eocene and Oligocene. *Nature* **446**, 176-179 (2007).

8 Larsen, H. C. *et al*. Seven million years of glaciation in Greenland. *Science* **264**, 952–955 (1994).

9 Thiede, J. *et al*. Millions of years of Greenland Ice Sheet history recorded in ocean sediments. *Polarforschung* **80**, 141-159 (2011).

10 Heisinger, B. *et al*. Production of selected cosmogenic radionuclides by muons. *Geochimica et Cosmochimica Acta* **66**, A558 (2002).

11 Portenga, E. & Bierman, P. R. Understanding Earth's eroding surface with ^{10}Be. *GSA Today* **21**, 4-10 (2011).

12 Lal, D. Cosmic ray labeling of erosion surfaces; in situ nuclide production rates and erosion models. *Earth and Planetary Science Letters* **104**, 424-439 (1991).

13 Alley, R. B., Clark, P. U., Huybrechts, P. & Joughin, I. Ice-Sheet and Sea-Level Changes. *Science* **310**, 456-460, doi:10.1126/science.1114613 (2005).

14 Lunt, D. J., Foster, G. L., Haywood, A. M. & Stone, E. J. Late Pliocene Greenland glaciation controlled by a decline in atmospheric CO_2 levels. *Nature* **454**, 1102-1105, doi:doi:10.1038/nature07223 (2008).

15 Hemming, S. R. Heinrich events: Massive late Pleistocene detritus layers of the North Atlantic and their global climate imprint. *Reviews of Geophysics* **42**, RG1005, doi:10.1029/2003rg000128 (2004).

16 Korschinek, G. *et al*. A new value for the half-life of ^{10}Be by Heavy-Ion Elastic Recoil Detection and liquid scintillation counting. *Nuclear Instruments and Methods in Physics Research B* **268**, 187-191, doi:10.1016/j.nimb.2009.09.020 (2010).

17 Nelson, A., Bierman, P. R., Shakun, J. D. & Rood, D. H. Using In situ cosmogenic ^{10}Be to identify the source of sediment leaving Greenland. *Earth Surface Processes and Landforms*, 164 (in press).

18 Funder, S. *et al*. Late Pliocene Greenland - The Kap Kobenhavn Formation in north Greenland. *Bulletin of the Geological Society of Denmark*, 117-134 (2001).

19 Clark, P. U. & Pollard, D. Origin of the Middle Pleistocene transition by ice sheet erosion of regolith. *Paleoceanography* **13**, 1–9 (1998).

20 Hansen, J. E. & Sato, M. in *Climate Change: Inferences from Paleoclimate and Regional Aspects* (eds A. Berger, Fedor Mesinger, & Djordje Sijacki) 21-48 (Springer, 2012).

21 Lawrence, K. T., Herbert, T. D., Brown, C. M., Raymo, M. E. & Haywood, A. M. High-amplitude variations in North Atlantic sea surface temperature during the early Pliocene warm period. *Paleoceanography* **24**, PA2218, doi:10.1029/2008pa001669 (2009).

22 de Vernal, A. & Hillaire-Marcel, C. Natural variability of Greenland climate, vegetation, and ice volume during the past million years. *Science* **320**, 1622–1625 (2008.).

23 Kohl, C. P. & Nishiizumi, K. Chemical isolation of quartz for measurement of *in-situ* -produced cosmogenic nuclides. *Geochimica et Cosmochimica Acta* **56**, 3583-3587 (1992).

24 Nishiizumi, K. *et al*. Absolute calibration of ^{10}Be AMS standards. *Nuclear Inst. and Methods in Physics Research, B* **258**, 403-413 (2007).

25 Jansen, E. *et al*. in *Climate Change 2007: The Physical Science Basis. Contribution of Working Group I to the Fourth Assessment Report of the Intergovernmental Panel on Climate Change* (eds S. Solomon *et al*.) 434-497 (Cambridge University Press, 2007).

26 Israelson, C. & Spezzaferri, S. in *Proceedings of the Ocean Drilling Program, Scientific Results* Vol. 152 (eds A.D. Saunders, H.C. Larsen, & S.W. Wise, Jr.) 233-241 (1998).

27 Fukuma, K. in *Proceedings of the Ocean Drilling Program, Scientific Results* Vol. 152 (eds A.D. Saunders, H.C. Larsen, & S.W. Wise, Jr.) 265-269 (1998).

28 Scholz, D. & Hoffmann, D. L. StalAge: An algorithm designed for construction of speleothem age models. *Quaternary Geochronology* **6**, 369-382, doi:http://dx.doi.org/10.1016/j.quageo.2011.02.002.

29 Lisiecki, L. & Raymo, M. A Pliocene-Pleistocene stack of 57 globally distributed benthic d18O records. *Paleoceanography* **20**, PA1003-1020, doi:doi:10.1029/2004PA001071 (2005).

Extended Data **TABLE 1.** Isotopic data and age model, Site 918

Sample	CAMS #	Top Depth (mbsf)	Bottom Depth (mbsf)	Top age (Ma)	Bottom age (Ma)	Blank corrected 10Be/9Be	quartz (g)	carrier 9Be (ug)	Measured 10Be (atoms/g)	Decay-corrected 10Be (atoms/g)
B504918-1	BE35206	0.5	6.1	0.012	0.141	8.44E-15 ± 4.47E-16	18.86	254.3	7601 ± 402	7898 ± 418
B507918-2	BE35234	6.3	11.3	0.149	0.224	9.32E-15 ± 7.72E-16	24.31	252.5	6463 ± 536	7095 ± 588
B504918-3	BE35207	11.9	18.5	0.249	0.331	2.77E-14 ± 1.47E-15	18.80	254.4	24991 ± 1325	28892 ± 1532
B507918-4	BE35235	19.4	25.4	0.367	0.456	3.05E-15 ± 2.70E-16	16.13	254.7	3211 ± 284	3944 ± 349
B504918-5	BE35208	25.8	32.3	0.475	0.558	1.14E-14 ± 5.65E-16	24.40	255.3	7958 ± 395	10302 ± 511
B507918-6	BE35237	32.8	36.3	0.561	0.615	6.27E-15 ± 4.56E-16	19.33	253.8	5494 ± 400	7372 ± 537
B507918-7	BE35238	36.9	41.3	0.625	0.689	1.86E-14 ± 6.30E-16	24.54	253.6	12849 ± 435	17843 ± 604
B505918-8	BE35211	41.8	44.3	0.691	0.745	8.17E-15 ± 4.05E-16	14.85	253.6	9308 ± 462	13326 ± 662
B507918-9	BE35239	45.0	45.6	0.748	0.762	4.17E-15 ± 3.13E-16	17.36	254.0	4072 ± 305	5938 ± 445
B505918-10	BE35212	47.3	50.6	0.911	1.019	1.96E-14 ± 7.71E-16	15.50	254.2	21409 ± 844	34676 ± 1367
B507918-11	BE35240	52.7	55.3	1.060	1.107	1.76E-14 ± 5.99E-16	19.93	254.2	14960 ± 510	25713 ± 876
B507918-12	BE35241	56.7	58.8	1.131	1.170	3.69E-14 ± 8.60E-16	19.96	252.9	31214 ± 728	55469 ± 1293
B505918-13	BE35213	59.0	68.3	1.172	1.339	1.48E-14 ± 6.00E-16	24.82	253.4	10063 ± 409	18849 ± 766
B505918-14	BE35214	69.7	86.7	1.363	1.811	1.65E-14 ± 5.89E-16	20.73	253.8	13501 ± 482	29842 ± 1065
B505918-15	BE35215	87.3	91.7	1.814	1.835	6.73E-15 ± 3.79E-16	10.22	254.1	11176 ± 630	27815 ± 1567
B505918-16	BE35216	96.3	96.9	1.857	1.859	1.33E-14 ± 5.12E-16	22.62	253.6	9939 ± 383	25157 ± 970
B505918-17	BE35217	98.3	116.0	1.866	1.953	2.59E-14 ± 7.60E-16	13.66	253.0	32054 ± 940	83251 ± 2441
B506918-17X	BE35233	98.3	116.0	1.866	1.953	2.19E-14 ± 1.01E-15	12.02	255.6	31072 ± 1432	80700 ± 3720
B505918-18	BE35218	117.8	147.3	1.964	2.137	1.84E-14 ± 6.16E-16	19.68	253.7	15833 ± 531	44114 ± 1479
B505918-19	BE35219	148.6	159.8	2.145	2.198	5.53E-15 ± 3.45E-16	15.31	254.0	6122 ± 382	18121 ± 1130
B506918-20	BE35222	161.1	168.8	2.201	2.206	4.90E-15 ± 4.11E-16	12.08	252.7	6841 ± 573	20573 ± 1724
B505918-21	BE35220	171.4	201.1	2.210	2.233	5.37E-15 ± 3.48E-16	8.49	253.6	10712 ± 693	32517 ± 2104
B506918-22	BE35224	204.3	232.5	2.242	2.369	2.64E-14 ± 7.34E-16	11.25	254.3	39927 ± 1108	126352 ± 3506
B506918-23	BE35225	233.2	251.0	2.378	2.551	1.25E-14 ± 5.70E-16	25.77	253.0	8217 ± 373	28157 ± 1279
B506918-24	BE35226	252.8	271.9	2.574	2.834	1.98E-15 ± 3.64E-16	11.23	253.9	2993 ± 549	11562 ± 2122
B506918-25	BE35227	273.6	316.3	2.856	3.499	5.12E-15 ± 4.95E-16	10.86	253.8	7990 ± 772	39103 ± 3779
B507918-26	BE35242	318.1	324.0	3.526	3.612	8.35E-15 ± 4.78E-16	14.78	254.1	9579 ± 549	57014 ± 3265
B506918-27	BE35228	386.6	405.2	4.529	4.806	3.36E-15 ± 4.55E-16	26.78	254.4	2134 ± 289	21993 ± 2976
B506918-28	BE35229	413.2	504.4	4.925	6.334	2.10E-15 ± 2.50E-16	10.47	253.9	3397 ± 404	56595 ± 6738
B506918-29	BE35230	504.7	543.1	6.334	9.491	1.32E-15 ± 2.11E-16	7.81	253.8	2875 ± 458	149907 ± 23874
B506918-30	BE35231	543.3	553.9	9.527	10.257	4.98E-15 ± 4.02E-16	25.30	253.4	3329 ± 269	466965 ± 37714

referenced to standard 07KNSTD3110[25] assuming a $^{10}Be/^{9}Be$ ratio of 2850 x 10^{-15}

Be extracted using the methods detailed in Corbett, L. Bierman, P., Graly, J., Neumann, T., Rood, D. (2013). Constraining landscape history and glacial erosivity using paired cosmogenic nuclides in Upernavik, Northwest Greenland. Geological Society of America Bulletin. v. 125, no. 9-10, 10.1130/B30813.1

Extended Data **TABLE 2.** 918 age model

Depth (mbsf)	Age (Ma)	error + (My)	error - (My)	Age constraint (Paleomag, Biostrat, 87Sr/86Sr)	Reference
0	0			Assumed modern	
10.26	0.4	0.6	0.6	0.709173	Israelson and Spezzaferri, 1998
10.26	0.3	0.7	0.6	0.709178	Israelson and Spezzaferri, 1998
16.26	0	0.8	0.6	0.709183	Israelson and Spezzaferri, 1998
36.01	0.6	0.5	0.6	0.709166	Israelson and Spezzaferri, 1998
45.9	0.78			Brunhes/Matuyama	Fukuma, 1998
49	0.99			Jaramillo top	Fukuma, 1998
52.9	1.07			Jaramillo bottom	Fukuma, 1998
58.07	0.9	0.5	0.6	0.709153	Israelson and Spezzaferri, 1998
71.1	1.39			hiatus	Fukuma, 1998
71.1	1.73			hiatus	Fukuma, 1998
81	1.79			Olduvai top	Fukuma, 1998
95.45	1	0.5	0.6	0.709145	Israelson and Spezzaferri, 1998
115.1	1.95			Olduvai bottom	Fukuma, 1998
146.8	2.14			Reunion top	Fukuma, 1998
154.77	1.7	0.9	0.5	0.709107	Israelson and Spezzaferri, 1998
162.41	1.9	1.7	0.6	0.709098	Israelson and Spezzaferri, 1998
162.41	1.9	1.7	0.6	0.709098	Israelson and Spezzaferri, 1998
168.76	1.1	0.6	0.5	0.709137	Israelson and Spezzaferri, 1998
184.97	1.3	0.6	0.5	0.709126	Israelson and Spezzaferri, 1998
209.67	1.8	1.1	0.6	0.709102	Israelson and Spezzaferri, 1998
221.55	2.7	2.3	1	0.709076	Israelson and Spezzaferri, 1998
246.57	1.9	1.8	0.6	0.709097	Israelson and Spezzaferri, 1998
246.57	2.3	2.4	0.7	0.709107	Israelson and Spezzaferri, 1998
273.06	2.7	2.3	1	0.709076	Israelson and Spezzaferri, 1998
280.47	2.6	2.3	0.9	0.709077	Israelson and Spezzaferri, 1998
320.56	4.4	0.9	2.3	0.709083	Israelson and Spezzaferri, 1998
485.15	5.8	0.6	0.6	0.709009	Israelson and Spezzaferri, 1998
485.15	6	0.6	0.6	0.709018	Israelson and Spezzaferri, 1998
485.4	6.3	0.6	0.6	0.709004	Israelson and Spezzaferri, 1998
486.9	6.2	0.5	0.6	0.709011	Israelson and Spezzaferri, 1998
495	3.94			Last occurrence R. gelida	Larsen, 1994
505.39	6.6	0.6	0.6	0.708992	Israelson and Spezzaferri, 1998
513	5.5			Last occurrence D. quinqueramus	Larsen, 1994
513	6.6			N. atlantica coiling chance (D to S)	Larsen, 1994
515.83	6.4	0.6	0.6	0.708979	Israelson and Spezzaferri, 1998
516.93	6.6	0.6	0.6	0.70897	Israelson and Spezzaferri, 1998
552.36	10.1	0.8	0.8	0.708927	Israelson and Spezzaferri, 1998
553.86	10.6	0.8	0.8	0.708915	Israelson and Spezzaferri, 1998
581.26	10	0.8	0.8	0.708931	Israelson and Spezzaferri, 1998
590.94	11	0.8	0.8	0.708903	Israelson and Spezzaferri, 1998
620.21	10.8	0.8	0.8	0.708908	Israelson and Spezzaferri, 1998
621.16	12	0.8	0.8	0.708878	Israelson and Spezzaferri, 1998
621.66	11.3	0.8	0.8	0.708894	Israelson and Spezzaferri, 1998
628	10.7			First occurrence N. acostanensis	Larsen, 1994
645	11.9			Last occurrence C. floridanus	Larsen, 1994
656.14	13.7	0.8	0.8	0.708832	Israelson and Spezzaferri, 1998
656.14	13.7	0.8	0.8	0.708833	Israelson and Spezzaferri, 1998
657	13.25	1.25	1.25	G. praemenardii range	Larsen, 1994
682.58	13.2	0.8	0.8	0.708846	Israelson and Spezzaferri, 1998
688	13.6			Last occurrence S. heteromorphus	Larsen, 1994
697.07	13	0.8	0.8	0.70885	Israelson and Spezzaferri, 1998
697.07	13.6	0.8	0.8	0.708835	Israelson and Spezzaferri, 1998
726.01	16.1	0.4	0.4	0.708757	Israelson and Spezzaferri, 1998
786.22	17.7	0.4	0.4	0.708647	Israelson and Spezzaferri, 1998
786.22	17.7	0.4	0.4	0.708648	Israelson and Spezzaferri, 1998
803.99	19.9	0.4	0.4	0.708496	Israelson and Spezzaferri, 1998
803.99	19.6	0.4	0.4	0.708519	Israelson and Spezzaferri, 1998
850.27	22.7	0.4	0.4	0.708303	Israelson and Spezzaferri, 1998
850.27	22.6	0.4	0.4	0.708314	Israelson and Spezzaferri, 1998
850.27	22.6	0.4	0.4	0.708311	Israelson and Spezzaferri, 1998

Israelson, C. & Spezzaferri, S. in *Proceedings of the Ocean Drilling Program, Scientific Results* **152** (eds A.D. Saunders, H.C. Larsen, & S.W. Wise, Jr.) 233-241 (1998).
Fukuma, K. in *Proceedings of the Ocean Drilling Program, Scientific Results* **152** (eds A.D. Saunders, H.C. Larsen, & S.W. Wise, Jr.) 265-269 (1998).
Larsen, H. C. *et al.* Seven million years of glaciation in Greenland. *Science* **264**, 952–955 (1994).

Extended Data **TABLE 3.** Grain size data data

Site	Hole	Core	Half	Section	Top	Bottom	Depth (mbsf)	Total dry mass (g)	>63 µm mass (g)	% coarse fraction
918	A	1	H	1	52	57	0.52	45.29	18.46	41%
918	A	1	H	1	95	100	0.95	32.39	6.84	21%
918	A	1	H	2	8	13	1.08	36.93	9.15	25%
918	A	1	H	2	42	47	1.42	49.22	9.83	20%
918	A	1	H	CC	0	5	1.60	49.59	4.34	9%
918	A	2	H	1	13	18	1.93	31.09	6.68	21%
918	A	2	H	1	55	60	2.35	47.14	5.52	12%
918	A	2	H	1	100	105	2.80	53.86	23.53	44%
918	A	2	H	1	142	147	3.22	31.24	4.82	15%
918	A	2	H	2	0	4	3.30	26.68	4.83	18%
918	A	2	H	2	53	57	3.83	31.29	2.94	9%
918	A	2	H	2	106	110	4.36	35.01	8.08	23%
918	A	2	H	2	146	150	4.76	40.63	8.09	20%
918	A	2	H	3	0	4	4.80	27.44	1.06	4%
918	A	2	H	3	52	56	5.32	47.39	15.33	32%
918	A	2	H	3	99	103	5.79	52.19	34.23	66%
918	A	2	H	3	134	137	6.14	44.12	29.45	67%
918	A	2	H	4	0	4	6.25	52.05	35.90	69%
918	A	2	H	4	53	57	6.78	46.32	6.88	15%
918	A	2	H	4	103	107	7.28	38.61	8.31	22%
918	A	2	H	4	146	150	7.71	40.57	5.97	15%
918	A	2	H	5	8	12	7.88	40.39	6.47	16%
918	A	2	H	5	50	54	8.30	30.87	3.19	10%
918	A	2	H	5	105	109	8.85	54.98	17.15	31%
918	A	2	H	5	146	150	9.26	51.97	32.70	63%
918	A	2	H	6	0	4	9.30	42.50	21.79	51%
918	A	2	H	6	56	60	9.86	55.92	24.27	43%
918	A	2	H	6	97	100	10.27	41.59	8.15	20%
918	A	2	H	7	0	4	10.30	40.69	7.72	19%
918	A	2	H	7	36	40	10.66	50.19	4.49	9%
918	A	2	H	CC	0	3	10.84	39.18	15.65	40%
918	A	3	H	1	0	5	11.30	27.91	5.48	20%
918	A	3	H	1	57	61	11.87	40.58	8.15	20%
918	A	3	H	2	0	4	11.95	32.92	7.84	24%
918	A	3	H	2	50	54	12.45	32.59	4.53	14%
918	A	3	H	2	96	100	12.91	39.65	3.36	8%
918	A	3	H	2	144	148	13.39	48.13	3.38	7%
918	A	3	H	3	0	4	13.45	34.90	3.51	10%
918	A	3	H	3	50	54	13.95	39.71	3.90	10%
918	A	3	H	3	91	95	14.36	37.36	2.58	7%
918	A	3	H	3	146	150	14.91	50.90	17.54	34%
918	A	3	H	4	0	4	14.95	50.54	24.93	49%
918	A	3	H	4	50	54	15.45	54.48	22.45	41%
918	A	3	H	4	96	100	15.91	38.90	6.48	17%
918	A	3	H	4	146	150	16.41	30.89	5.68	18%
918	A	3	H	5	0	4	16.45	34.63	7.48	22%
918	A	3	H	5	50	54	16.95	34.87	7.39	21%
918	A	3	H	5	100	104	17.45	52.23	21.00	40%
918	A	3	H	5	146	150	17.91	37.34	12.04	32%
918	A	3	H	6	0	4	17.95	40.70	14.51	36%
918	A	3	H	6	50	54	18.45	45.36	10.72	24%
918	A	3	H	6	107	111	19.02	31.83	18.48	58%
918	A	3	H	6	146	150	19.41	49.28	10.37	21%
918	A	3	H	7	0	5	19.45	45.77	25.44	56%
918	A	3	H	7	50	54	19.95	50.51	9.70	19%
918	A	3	H	CC	0	5	20.10	58.65	16.69	28%
918	A	4	H	1	4	8	20.84	31.98	4.76	15%
918	A	4	H	1	50	54	21.30	64.72	11.86	18%
918	A	4	H	1	103	107	21.83	54.89	1.26	2%
918	A	4	H	1	146	150	22.26	42.09	3.36	8%
918	A	4	H	2	0	4	22.30	49.09	4.42	9%
918	A	4	H	2	50	54	22.80	57.39	23.70	41%
918	A	4	H	2	100	104	23.30	62.32	9.59	15%
918	A	4	H	2	146	150	23.76	46.05	13.18	29%
918	A	4	H	3	0	4	23.80	33.17	10.00	30%

Extended Data **TABLE 3.** Grain size data data

Site	Hole	Core	Half	Section	Top	Bottom	Depth (mbsf)	Total dry mass (g)	>63 µm mass (g)	% coarse fraction
918	A	4	H	3	50	54	24.30	31.95	1.33	4%
918	A	4	H	3	100	104	24.80	36.09	1.57	4%
918	A	4	H	3	145	150	25.25	41.89	23.81	57%
918	A	4	H	4	12	16	25.42	57.37	24.15	42%
918	A	4	H	4	50	54	25.80	60.63	9.11	15%
918	A	4	H	4	102	106	26.32	55.21	24.27	44%
918	A	4	H	4	140	145	26.70	49.99	7.73	15%
918	A	4	H	5	10	14	26.90	51.97	8.34	16%
918	A	4	H	5	50	54	27.30	60.09	5.43	9%
918	A	4	H	5	105	109	27.85	56.51	6.83	12%
918	A	4	H	5	146	150	28.26	50.64	7.32	14%
918	A	4	H	6	0	4	28.30	34.95	4.81	14%
918	A	4	H	6	50	54	28.80	36.20	11.58	32%
918	A	4	H	6	105	109	29.35	42.67	9.12	21%
918	A	4	H	6	146	150	29.76	46.07	1.98	4%
918	A	4	H	7	0	4	29.80	40.57	3.66	9%
918	A	4	H	7	45	49	30.25	43.88	6.08	14%
918	A	4	H	CC	18	22	30.47	33.54	4.95	15%
918	A	5	H	1	0	4	30.30	25.64	3.44	13%
918	A	5	H	1	53	57	30.83	39.90	20.63	52%
918	A	5	H	1	105	109	31.35	29.20	8.91	31%
918	A	5	H	1	146	150	31.76	54.66	8.77	16%
918	A	5	H	2	0	4	31.80	54.42	22.29	41%
918	A	5	H	2	50	54	32.30	50.46	25.54	51%
918	A	5	H	2	100	104	32.80	42.40	15.37	36%
918	A	5	H	2	146	150	33.26	55.39	2.34	4%
918	A	5	H	3	0	4	33.30	46.01	2.98	6%
918	A	5	H	3	48	52	33.78	51.07	0.86	2%
918	A	5	H	3	98	102	34.28	66.13	32.87	50%
918	A	5	H	3	146	150	34.76	56.59	34.02	60%
918	A	5	H	4	0	4	34.80	59.99	26.84	45%
918	A	5	H	4	50	54	35.30	59.30	20.96	35%
918	A	5	H	4	100	104	35.80	54.88	28.19	51%
918	A	5	H	4	146	150	36.26	53.99	22.58	42%
918	A	5	H	5	0	4	36.30	54.95	22.30	41%
918	A	5	H	5	57	61	36.87	46.24	3.48	8%
918	A	5	H	5	104	108	37.34	47.66	19.96	42%
918	A	5	H	5	146	150	37.76	42.82	6.79	16%
918	A	5	H	6	0	4	37.80	34.70	17.80	51%
918	A	5	H	6	50	54	38.30	41.34	17.84	43%
918	A	5	H	6	95	99	38.75	38.32	23.85	62%
918	A	5	H	6	140	143	39.20	31.94	4.54	14%
918	A	5	H	7	0	4	39.30	23.62	4.85	21%
918	A	5	H	7	51	55	39.81	51.71	3.48	7%
918	A	5	H	CC	0	4	39.85	46.47	4.70	10%
918	A	6	H	1	0	4	39.80	36.50	10.69	29%
918	A	6	H	1	46	50	40.26	31.59	8.02	25%
918	A	6	H	1	102	106	40.82	53.46	27.19	51%
918	A	6	H	1	147	150	41.27	45.15	18.44	41%
918	A	6	H	2	0	4	41.30	31.81	18.92	59%
918	A	6	H	2	50	54	41.80	37.56	9.27	25%
918	A	6	H	2	96	100	42.26	48.52	20.20	42%
918	A	6	H	2	146	150	42.76	56.33	24.64	44%
918	A	6	H	3	0	4	42.80	45.76	28.81	63%
918	A	6	H	3	50	54	43.30	37.74	11.34	30%
918	A	6	H	3	92	96	43.72	28.63	3.29	11%
918	A	6	H	3	146	150	44.26	36.02	21.68	60%
918	A	6	H	4	72	86	45.02	210.10	188.19	90%
918	A	6	H	4	132	146	45.62	168.19	129.79	77%
918	A	6	H	6	0	20	47.30	187.89	75.16	40%
918	A	6	H	6	132	150	48.62	141.06	6.96	5%
918	A	6	H	CC	0	14	49.53	142.34	26.75	19%
918	A	7	H	1	132	150	50.62	209.27	67.49	32%
918	A	7	H	3	36	50	52.66	239.63	116.67	49%
918	A	7	H	3	136	150	53.66	225.85	47.19	21%

Extended Data **TABLE 3.** Grain size data data

Site	Hole	Core	Half	Section	Top	Bottom	Depth (mbsf)	Total dry mass (g)	>63 µm mass (g)	% coarse fraction
918	A	7	H	5	0	15	55.30	218.56	11.55	5%
918	A	7	H	5	136	150	56.66	218.44	87.00	40%
918	A	7	H	7	0	14	58.30	191.88	76.53	40%
918	A	7	H	7	53	67	58.83	179.13	50.62	28%
918	A	7	H	CC	0	15	58.97	141.86	23.44	17%
918	A	8	H	2	0	15	60.30	179.54	71.59	40%
918	A	8	H	2	136	150	61.66	153.60	3.29	2%
918	A	8	H	4	0	14	63.30	143.13	8.71	6%
918	A	8	H	4	136	150	64.66	139.77	3.40	2%
918	A	8	H	6	0	14	66.30	167.36	24.94	15%
918	A	8	H	6	136	150	67.66	173.95	25.31	15%
918	A	9	H	1	0	14	68.30	130.50	19.98	15%
918	A	9	H	1	136	150	69.66	165.52	36.38	22%
918	A	9	H	3	14	28	71.44	172.19	8.04	5%
918	A	9	H	3	136	150	72.66	177.21	28.27	16%
918	A	9	H	5	0	14	74.30	150.47	5.86	4%
918	A	9	H	5	136	150	75.66	160.08	6.97	4%
918	A	9	H	7	0	14	77.30	136.16	1.00	1%
918	A	9	H	CC	0	14	77.96	188.16	6.02	3%
918	A	10	H	2	0	14	79.30	164.19	61.49	37%
918	A	10	H	2	136	150	80.66	137.10	15.88	12%
918	A	10	H	4	0	14	82.30	163.83	5.02	3%
918	A	10	H	4	131	145	83.61	158.64	7.52	5%
918	A	10	H	6	0	14	85.30	154.60	5.27	3%
918	A	10	H	6	136	150	86.66	169.30	28.59	17%
918	A	11	H	1	0	14	87.30	180.92	22.89	13%
918	A	11	H	1	136	150	88.66	182.68	61.98	34%
918	A	11	H	3	0	14	90.30	215.14	54.35	25%
918	A	11	H	3	136	150	91.66	128.47	5.96	5%
918	A	11	H	7	0	14	96.30	169.04	119.73	71%
918	A	11	H	7	56	70	96.86	205.25	149.43	73%
918	A	12	H	2	0	4	98.30	149.81	8.51	6%
918	A	12	H	2	134	148	99.64	168.03	3.30	2%
918	A	12	H	4	4	18	101.34	169.58	2.57	2%
918	A	12	H	4	34	48	101.64	176.51	3.09	2%
918	A	12	H	6	0	14	104.30	158.43	2.60	2%
918	A	12	H	6	83	97	105.13	225.81	1.00	0%
918	A	13	H	1	0	14	106.30	118.34	0.71	1%
918	A	13	H	1	134	148	107.64	148.80	0.80	1%
918	A	13	H	3	0	14	109.30	144.61	1.94	1%
918	A	13	H	3	131	145	110.61	139.34	1.49	1%
918	A	13	H	5	15	29	112.45	186.12	52.52	28%
918	A	13	H	5	113	127	113.43	171.82	78.17	45%
918	A	13	H	7	0	14	115.30	169.80	18.96	11%
918	A	13	H	CC	0	14	115.97	182.53	14.07	8%
918	A	14	H	2	53	67	117.83	234.04	19.44	8%
918	A	14	H	2	127	145	118.57	213.01	11.55	5%
918	A	14	H	5	0	14	121.80	203.48	0.79	0%
918	A	14	H	5	118	132	122.98	174.35	0.79	0%
918	A	15	H	2	0	14	126.80	218.26	11.39	5%
918	A	15	H	2	136	150	128.16	206.99	18.02	9%
918	A	15	H	5	0	20	131.30	290.66	34.87	12%
918	A	15	H	5	130	150	132.60	229.08	19.40	8%
918	A	16	H	2	0	14	134.80	211.96	5.01	2%
918	A	16	H	2	130	150	136.10	280.12	11.46	4%
918	A	16	H	5	0	14	139.30	144.75	9.11	6%
918	A	16	H	5	136	150	140.66	165.88	17.24	10%
918	A	17	H	1	44	58	143.24	159.85	12.79	8%
918	A	17	H	1	133	147	144.13	187.78	12.66	7%
918	A	17	H	4	0	20	147.30	203.93	19.98	10%
918	A	17	H	4	134	148	148.64	174.27	17.20	10%
918	A	17	H	7	0	14	151.80	226.92	22.88	10%
918	A	17	H	CC	0	14	152.30	162.82	5.26	3%
918	A	18	H	3	0	14	155.30	195.82	36.45	19%
918	A	18	H	3	104	124	156.34	290.67	73.75	25%

Extended Data **TABLE 3.** Grain size data data

Site	Hole	Core	Half	Section	Top	Bottom	Depth (mbsf)	Total dry mass (g)	>63 µm mass (g)	% coarse fraction
918	A	18	H	6	0	14	159.80	184.27	59.80	32%
918	A	18	H	6	133	147	161.13	181.83	47.76	26%
918	A	19	H	2	0	14	163.30	197.30	48.35	25%
918	A	19	H	2	131	145	164.61	201.10	27.92	14%
918	A	19	H	5	0	14	167.80	192.30	3.50	2%
918	A	19	H	5	102	116	168.82	237.12	63.67	27%
918	A	20	X	1	10	24	171.40	142.38	11.35	8%
918	A	20	X	1	131	145	172.61	130.24	14.98	12%
918	A	20	X	4	67	81	176.47	187.76	25.55	14%
918	A	20	X	CC	0	14	176.98	142.55	12.44	9%
918	A	21	X	1	50	64	182.00	181.42	12.43	7%
918	A	21	X	1	120	140	182.70	188.37	10.36	5%
918	A	21	X	3	0	14	184.50	159.29	22.70	14%
918	A	21	X	3	90	104	185.40	170.98	46.99	27%
918	A	22	X	1	23	37	191.13	142.21	2.87	2%
918	A	22	X	1	76	90	191.66	149.56	1.91	1%
918	A	23	X	1	0	14	199.80	212.76	16.74	8%
918	A	23	X	1	128	142	201.08	148.70	5.20	3%
918	A	23	X	4	0	14	204.30	162.80	18.34	11%
918	A	23	X	4	124	138	205.54	155.62	51.86	33%
918	A	24	X	1	10	24	208.80	133.12	8.81	7%
918	A	24	X	1	133	147	210.03	171.38	10.72	6%
918	A	24	X	4	0	14	213.20	158.98	13.01	8%
918	A	24	X	4	132	146	214.52	129.92	4.72	4%
918	A	24	X	7	0	14	217.20	142.44	29.31	21%
918	A	24	X	CC	0	14	217.86	148.85	18.43	12%
918	A	25	X	3	5	19	220.65	148.70	4.64	3%
918	A	25	X	3	132	146	221.92	179.31	15.75	9%
918	A	25	X	6	3	17	225.13	168.54	7.09	4%
918	A	25	X	6	132	146	226.42	157.51	7.75	5%
918	A	26	X	2	0	14	228.00	153.67	2.98	2%
918	A	26	X	2	132	146	229.32	147.60	2.14	1%
918	A	26	X	5	0	14	232.50	139.82	5.34	4%
918	A	26	X	5	74	88	233.24	138.88	4.94	4%
918	A	27	X	2	0	14	236.70	151.80	15.57	10%
918	A	27	X	2	134	148	238.04	158.12	20.23	13%
918	A	27	X	5	0	14	241.20	154.72	6.31	4%
918	A	27	X	5	133	147	242.53	168.81	15.51	9%
918	A	28	X	2	0	14	245.60	144.68	1.74	1%
918	A	28	X	2	120	134	246.80	131.26	10.81	8%
918	A	28	X	5	0	14	250.10	184.06	65.35	36%
918	A	28	X	CC	0	14	251.03	193.55	71.52	37%
918	A	29	X	1	0	14	252.80	140.80	61.48	44%
918	A	29	X	1	99	103	253.79	222.06	109.63	49%
918	A	31	X	1	2	16	270.62	127.25	16.81	13%
918	A	31	X	1	133	147	271.93	141.82	9.78	7%
918	A	31	X	3	0	14	273.60	142.42	18.71	13%
918	A	31	X	3	110	124	274.70	129.16	42.86	33%
918	A	31	X	5	0	14	276.60	146.59	2.81	2%
918	A	31	X	5	133	147	277.93	141.80	6.52	5%
918	A	32	X	1	49	63	279.99	99.94	6.38	6%
918	A	32	X	1	123	137	280.73	143.26	10.45	7%
918	A	33	X	1	51	65	288.91	154.11	23.08	15%
918	A	33	X	1	133	147	289.73	137.38	4.31	3%
918	A	33	X	2	19	32	290.09	123.64	5.96	5%
918	A	33	X	2	63	77	290.53	126.20	10.71	8%
918	A	35	X	1	21	35	306.41	124.00	23.12	19%
918	A	37	X	1	0	14	315.10	147.88	22.01	15%
918	A	37	X	1	121	135	316.31	132.62	12.70	10%
918	A	37	X	3	0	14	318.10	169.08	33.11	20%
918	A	37	X	3	133	147	319.43	169.49	33.46	20%
918	A	37	X	5	0	14	321.10	164.42	44.58	27%
918	A	37	X	5	70	84	321.80	141.12	20.57	15%
918	A	38	X	CC	8	22	323.98	172.45	72.66	42%
918	D	11	R	1	46	64	386.56	149.39	53.53	36%

Extended Data **TABLE 3.** Grain size data data

Site	Hole	Core	Half	Section	Top	Bottom	Depth (mbsf)	Total dry mass (g)	>63 µm mass (g)	% coarse fraction
918	D	11	R	1	98	122	387.08	152.13	59.11	39%
918	D	13	R	1	33	47	404.23	177.10	47.90	27%
918	D	13	R	1	132	146	405.22	158.13	45.14	29%
918	D	14	R	1	43	57	413.23	118.01	7.32	6%
918	D	14	R	1	136	150	414.16	141.61	16.51	12%
918	D	14	R	2	10	28	414.40	131.50	5.17	4%
918	D	14	R	2	97	111	415.27	120.30	4.51	4%
918	D	22	R	1	13	37	483.93	245.54	20.23	8%
918	D	22	R	1	120	134	485.00	129.67	13.28	10%
918	D	22	R	2	35	49	485.65	209.27	36.15	17%
918	D	22	R	2	103	117	486.33	196.31	17.00	9%
918	D	24	R	3	68	81	506.72	96.94	4.28	4%
918	D	25	R	1	14	28	512.94	129.46	25.75	20%
918	D	25	R	1	65	79	513.45	147.18	4.85	3%
918	D	25	R	2	31	45	514.11	173.02	3.60	2%
918	D	25	R	3	0	17	514.37	192.26	4.87	3%
918	D	25	R	3	134	148	515.71	155.15	17.06	11%
918	D	25	R	4	0	19	515.94	180.93	10.40	6%
918	D	25	R	4	86	100	516.80	113.53	3.81	3%
918	D	25	R	5	37	51	517.31	123.93	8.91	7%
918	D	25	R	5	63	76	517.57	172.60	15.76	9%
918	D	27	R	1	7	21	532.17	145.68	8.17	6%
918	D	27	R	1	81	95	532.91	117.89	6.24	5%
918	D	27	R	2	0	14	533.60	160.98	14.68	9%
918	D	27	R	2	125	139	534.85	155.01	7.13	5%
918	D	27	R	3	15	29	535.25	146.53	10.18	7%
918	D	27	R	3	105	119	536.15	110.00	5.21	5%
918	D	28	R	1	13	27	541.93	120.88	4.49	4%
918	D	28	R	1	125	139	543.05	160.01	4.58	3%
918	D	28	R	2	0	31	543.30	241.71	48.87	20%
918	D	28	R	2	122	150	544.52	259.58	4.72	2%
918	D	28	R	3	0	14	544.80	139.03	1.78	1%
918	D	28	R	3	126	140	546.06	146.27	6.66	5%
918	D	28	R	4	10	24	546.40	139.68	3.21	2%

Extended Data **TABLE 4.** Blank data, ^{10}Be

Sample	CAMS #	Blank 10Be/9Be	carrier 9Be (ug)
B504BLKX	BE35209	4.41E-16 ± 1.01E-16	253.9
B505BLK	BE35210	5.77E-16 ± 1.33E-16	251.7
B505BLKX	BE35221	3.39E-16 ± 1.44E-16	255.6
B506BLK	BE35223	3.91E-16 ± 9.66E-17	254.1
B507BLK	BE35236	5.81E-16 ± 1.49E-16	253.8
B506BLKX	BE35232	4.10E-16 ± 2.32E-16	253.4
	AVERAGE (1 SD)	4.57E-16 ± 1.00E-16	

referenced to standard 07KNSTD3110[25] assuming a $^{10}Be/^{9}Be$ ratio of 2850 x 10^{-15}

Extended Data **TABLE 5.** Stable isotope data

Site	Hole	Core	Half	Section	Top	Bottom	Depth (mbsf)	d13C	d18O
918	A	1	H	2	0	2	1	-0.03	4.22
918	A	1	H	2	50	52	1.5	-0.31	4.56
918	A	2	H	1	20	22	2	-0.24	4.61
918	A	2	H	1	70	72	2.5	-0.33	4.56
918	A	2	H	1	120	122	3	-0.15	4.53
918	A	2	H	2	20	22	3.5	-0.07	4.31
918	A	2	H	2	120	122	4	0.12	4.43
918	A	2	H	3	20	22	5	-0.17	4.28
918	A	2	H	3	70	72	5.5	-0.14	4.13
918	A	2	H	3	120	122	6	0.04	3.84
918	A	2	H	4	25	27	6.5	0.09	3.82
918	A	2	H	4	75	77	7	-0.13	4.11
918	A	2	H	4	125	127	7.5	-0.80	3.58
918	A	2	H	5	20	22	8	-0.04	4.25
918	A	2	H	5	70	72	8.5	0.12	4.09
918	A	2	H	5	120	122	9	0.21	4.14
918	A	2	H	6	20	22	9.4	0.26	4.22
918	A	2	H	6	60	22	9.5	0.24	4.01
918	A	2	H	7	20	22	10.54	0.12	4.15
918	A	2	H	CC	3	5	10.94	0.46	4.32
918	A	3	H	1	20	22	12	0.10	4.04
918	A	3	H	2	55	57	12.5	-0.27	3.75
918	A	3	H	2	105	107	13	-0.36	3.92
918	A	3	H	2	149	151	13.44	-0.60	3.76
918	A	3	H	3	55	57	14	0.13	4.27
918	A	3	H	4	5	7	15	0.44	4.07
918	A	3	H	4	105	107	16	-0.20	3.63
918	A	3	H	5	5	7	16.5	-0.03	4.21
918	A	3	H	5	55	57	17	-0.12	3.81
918	A	3	H	5	105	107	17.5	0.14	4.03
918	A	3	H	6	5	7	18	-0.13	4.59
918	A	3	H	6	55	57	18.5	-0.16	4.27
918	A	3	H	6	105	107	19	0.35	3.55
918	A	3	H	7	5	7	19.35	-0.17	4.29
918	A	3	H	7	40	42	19.5	-0.35	4.55
918	A	4	H	1	20	22	21	-0.71	4.44
918	A	4	H	1	70	72	21.5	-0.65	4.52
918	A	4	H	1	120	122	22	-1.08	4.76
918	A	4	H	2	20	22	22.5	-1.05	4.44
918	A	4	H	2	70	72	23	-0.60	4.44
918	A	4	H	2	120	122	23.5	-1.06	4.23
918	A	4	H	3	21	23	24	-0.65	4.04
918	A	4	H	3	70	72	24.5	-0.59	3.76
918	A	4	H	3	120	122	25	-0.87	4.38
918	A	4	H	4	20	22	25.5	-1.06	4.03
918	A	4	H	4	70	72	26	-0.52	4.10

Extended Data **TABLE 5.** Stable isotope data

Site	Hole	Core	Half	Section	Top	Bottom	Depth (mbsf)	d13C	d18O
918	A	4	H	4	120	122	26.5	-0.82	4.19
918	A	4	H	5	20	22	27	-0.56	4.06
918	A	4	H	5	70	72	27.5	-0.38	3.95
918	A	4	H	5	120	122	28	-0.51	4.24
918	A	4	H	6	20	22	28.5	-0.76	4.44
918	A	4	H	6	70	72	29	-0.47	4.28
918	A	4	H	6	120	122	29.5	-0.54	3.89
918	A	4	H	7	27	29	30.07	-0.35	4.00
918	A	5	H	1	20	22	30.5	-0.25	3.66
918	A	5	H	1	70	72	31	-0.38	3.79
918	A	5	H	2	5	7	31.85	0.23	4.12
918	A	5	H	2	20	22	32	-0.49	3.76
918	A	5	H	2	71	73	32.51	-0.64	3.74
918	A	5	H	2	120	122	33	-1.13	3.96
918	A	5	H	3	71	73	34.5	-0.77	3.62
918	A	5	H	4	20	22	35	-0.39	4.05
918	A	5	H	4	71	73	35.51	0.02	4.10
918	A	5	H	4	120	122	36	-0.16	4.21
918	A	5	H	5	71	73	37	-0.31	4.42
918	A	5	H	5	120	122	37.5	-0.76	4.10
918	A	5	H	6	20	22	38	-0.08	4.40
918	A	5	H	6	70	72	38.5	-0.78	4.14
918	A	5	H	6	120	122	39	-2.18	4.20
918	A	5	H	7	41	43	39.71	-1.70	3.97
918	A	6	H	1	120	122	41	-0.41	4.17
918	A	6	H	2	20	22	41.5	-0.19	4.30
918	A	6	H	2	70	72	42	-0.02	4.12
918	A	6	H	3	20	22	43	-0.27	4.05
918	A	6	H	3	70	72	43.5	0.10	4.19
918	A	6	H	3	120	122	44	-0.30	3.76
918	A	6	H	4	20	22	44.5	-0.41	4.20
918	A	6	H	4	70	72	45	-0.42	4.24
918	A	6	H	5	20	22	46	0.08	3.56
918	A	6	H	5	120	122	47	-0.03	4.05

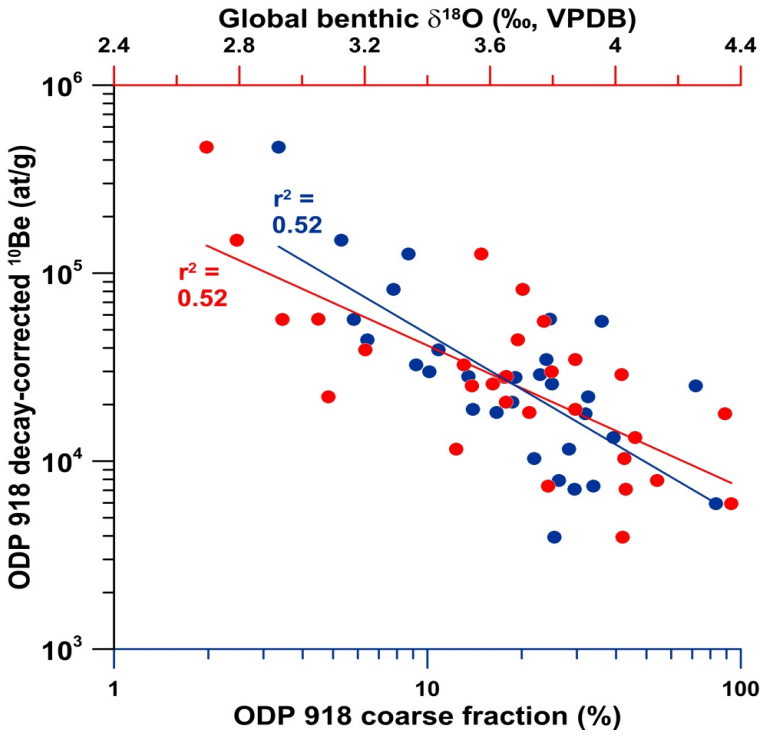

Extended Data Figure 4. The decay-corrected ^{10}Be record (Figure 3c) regressed against the site 918 coarse fraction record (Figure 3b) (blue) and the marine benthic d18O record (Figure 3d) (red) over the past 10 Myr. The coarse fraction and benthic d18O data were averaged in bins spanning the age ranges of corresponding ^{10}Be measurements. Best-fit lines and regression statistics are shown. Note that the ^{10}Be and coarse fraction axes are log-scale.